

PREPARED FOR SUBMISSION TO JCAP

# The Sommerfeld Enhancement in the Scotogenic Model with Large Electroweak Scalar Multiplets

Talal Ahmed Chowdhury<sup>a</sup> & Salah Nasri<sup>b</sup>

<sup>a</sup>Department of Physics, University of Dhaka, P.O. Box 1000, Dhaka, Bangladesh

<sup>b</sup>Department of Physics, UAE University, P.O. Box 17551, Al-Ain, United Arab Emirates

E-mail: [talal@du.ac.bd](mailto:talal@du.ac.bd), [snasri@uaeu.ac.ae](mailto:snasri@uaeu.ac.ae)

**Abstract.** We investigate the Sommerfeld enhancement (SE) in the generalized scotogenic model with large electroweak multiplets. We focus on scalar dark matter (DM) candidate of the model and compare DM annihilation cross sections to  $WW$ ,  $ZZ$ ,  $\gamma\gamma$  and  $\gamma Z$  at present day in the galactic halo for scalar doublet and its immediate generalization, the quartet in their respective viable regions of parameter space. We find that larger multiplet has sizable Sommerfeld enhanced annihilation cross section compared to the doublet and because of that it is more likely to be constrained by the current H.E.S.S. results and future CTA sensitivity limits.

---

## Contents

<b>1</b>	<b>Introduction</b>	<b>1</b>
<b>2</b>	<b>The Model</b>	<b>2</b>
2.1	The Scalar Potential and the Particle states	3
2.2	Scalar Dark Matter	4
<b>3</b>	<b>Sommerfeld Enhancement with large Electroweak Scalar Multiplets</b>	<b>5</b>
3.1	The 2-particle states, potential and annihilation matrix	5
3.1.1	The 2-particle states	5
3.1.2	The Potential and Annihilation Matrix	5
3.2	Sommerfeld enhanced annihilation cross section	7
<b>4</b>	<b>Result and Discussion</b>	<b>8</b>
4.1	DM constraints and allowed parameter space	8
4.2	Sommerfeld enhanced Cross sections	12
4.2.1	$SS \rightarrow WW$	12
4.2.2	$SS \rightarrow ZZ$	13
4.2.3	$SS \rightarrow \gamma\gamma \& \gamma Z$	13
4.3	Discussion	14
<b>5</b>	<b>Conclusion and outlook</b>	<b>18</b>
<b>A</b>	<b>The Potential and Annihilation Matrix Elements</b>	<b>20</b>
A.1	NR Limit	20
A.2	The Potential Matrix elements	21
A.3	The Annihilation Matrix Elements	23

---

## 1 Introduction

Though considerable amount of astrophysical and cosmological studies suggest the Dark Matter (DM) to be an essential component of our universe, its conclusive particle nature is yet to be determined. Therefore currently the extensive searches for the DM have been carried out using various direct and indirect detection methods. While the direct detection mainly looks for the DM-nucleus scattering in the detector, the indirect detection focuses on the search of atypical  $e^+$ ,  $\bar{p}$ ,  $\gamma$  and  $\nu$  signatures of extraterrestrial origin i.e. from DM-DM annihilation or decay in the universe, using ground and satellite based detectors. In recent years, the gamma-ray observation by Cherenkov telescope has provided stringent and robust constraints [1–5] and it is also reaching the sensitivity level of DM annihilation cross sections to different final states of the Standard Model (SM) particles for the DM in  $O(1 - 100)$  TeV mass range [6, 9]. As a result, the present constraints and sensitivity limits, such as the latest result of H.E.S.S. (High Energy Stereoscopic System) for searching DM annihilation towards the inner galactic halo [7, 8] and the projected reach of CTA (Cherenkov Telescope Array) [10–13], can allow one to investigate the viability of a particular DM model with TeV mass with respect to current observation and upcoming experiments.

Why is the TeV mass-ranged DM in the focus of the indirect detection? When the DM with mass  $m_{\text{DM}} \gg m_W$ , is charged under the SM gauge group  $SU(2)_L \times U(1)_Y$  and non-relativistic, its annihilation cross section and hence the indirect detection rate is affected by a non-perturbative correction known as the Sommerfeld enhancement (SE). The SE, first discovered in the study of very slow electron scattering [14], has gained much focus in the context of DM phenomenology [15–42] (and references therein). In the case of non-relativistic DM with electroweak quantum numbers and TeV mass, the gauge boson exchange between two DM particles will induce long ranged attractive (repulsive) force which in turn modifies the incoming asymptotic plane waves and greatly enhances (suppresses) the annihilation cross section than the typical tree-level or loop-induced cross section. Thus, such enhancement can substantially increase the detection prospects of the DM annihilation in the Cherenkov telescopes or in satellites.

The Scotogenic model [43] is a well-motivated model which not only provides fermionic and/or scalar dark matter candidates (depending on region of parameter space) but also generates the neutrino mass radiatively at one loop [44–50]. As there is no symmetry reason to prevent extending the scotogenic model with scalars and fermions of larger  $SU(2)_L$  representations, in its generalized version, the scalar doublet and singlet fermion of the minimal model can be replaced by an even dimensional  $(J, Y) = (n/2, 1/2)$  electroweak scalar multiplet and corresponding odd dimensional (either  $(J, Y) = (\frac{n-1}{2}, 0)$  or  $(J, Y) = (\frac{n+1}{2}, 0)$ ) fermionic multiplets [51–57]. For the generalized scotogenic model, SE is expected to be significantly large compared to the minimal one as more states of larger electroweak multiplets will contribute to the enhancement which is the main focus of this investigation. The SE analysis of the fermionic DM in the scotogenic model resembles that of well-studied fermionic minimal dark matter model [20, 21, 58]. For this reason, we are not going to pursue fermionic DM in this study and instead we will focus on the case of scalar DM. The indirect detection prospects of the scalar DM of the minimal scotogenic model have been addressed in the light of H.E.S.S. results and upcoming CTA limits in [59, 60]. As the scalar doublet and higher multiplet have the same set of parameters, we will carry out a comparative study of SE for the scalar doublet and its immediate generalization, the quartet  $(J, Y) = (3/2, 1/2)$  representation [61] in their respective viable regions of parameter space and see how much SE increases for larger multiplets.

The article is organized as follows. In section 2, we present the model and set up the notation for subsequent analysis. In section 3, we briefly sketch the 2-particle states, potential and annihilation matrix and present the Schrodinger equation to calculate Sommerfeld enhancement for scalar multiplet in the generalized scotogenic model. In section 4, we present the Sommerfeld enhanced DM annihilation cross sections for the doublet and the quartet cases and discuss their implications in the light of H.E.S.S. results and CTA sensitivity limits. We conclude in section 5. In appendix A, we present the non-relativistic limit of scalar components, 2-particle effective action, the potential and  $S$ -wave annihilation matrix elements of the generalized scotogenic model.

## 2 The Model

The scalar sector of the generalized scotogenic model has been presented in [55, 61]. Here we briefly present the potential and the particle states for setting up our notations.

## 2.1 The Scalar Potential and the Particle states

The general Higgs-scalar potential that involves the  $SU(2)_L$  scalar multiplet  $\Delta$  with isospin,  $J = n/2$  ( $n$  odd) and hyper-charge,  $Y = 1/2$ , symmetric under a  $Z_2$ , is as follows,

$$V_0(H, \Delta) = -\mu^2 H^\dagger H + M_0^2 \Delta^\dagger \Delta + \lambda_1 (H^\dagger H)^2 + \lambda_2 (\Delta^\dagger \Delta)^2 + \lambda_3 |\Delta^\dagger T^a \Delta|^2 \\ + \alpha H^\dagger H \Delta^\dagger \Delta + \beta H^\dagger \tau^a H \Delta^\dagger T^a \Delta + \gamma \left[ (H^T \epsilon \tau^a H) (\Delta^T C T^a \Delta)^\dagger + h.c \right] \quad (2.1)$$

Here,  $\tau^a$  and  $T^a$  are the  $SU(2)$  generators in fundamental and  $\Delta$ 's representation respectively.  $C$  is an antisymmetric matrix such that  $CT^a C^{-1} = -T^{aT}$ . As  $C$  is antisymmetric, it can only be defined for even dimensional space, i.e only for half-integer representation. If the isospin of the representation is  $J$  then  $C$  is  $(2J+1) \times (2J+1)$  dimensional matrix. The generators are defined so that they satisfy  $Tr[\tau^a \tau^b] = \frac{1}{2} \delta^{ab}$  for fundamental representation and  $Tr[\tau^a \tau^b] = D_2(\Delta) \delta^{ab}$  for  $\Delta$ 's representation where  $D_2(\Delta)$  is the Dynkin index of  $\Delta$ . In addition, the  $\gamma$  term is only allowed for representations with  $(J, Y) = (\frac{n}{2}, \frac{1}{2})$  and it is essential for the mass splitting between scalar and pseudoscalar components in the neutral field of the scalar multiplet in a renormalizable way.

Incidentally for complex odd dimensional ( $J = n, Y \neq 0$ ), ( $n = 1, 2, \dots$ ) scalar multiplets,  $\gamma$  term doesn't occur in the  $Z_2$  symmetric scalar potential Eq.(2.1) and no mass splitting takes place between  $S$  and  $A$  of the neutral component [28]. But higher dimensional operators [62] such as

$$O_\delta \sim \frac{c}{\Lambda^2} \Delta \Delta H^* H^* H^* H^* + h.c \quad (2.2)$$

where  $\Delta$  can be ( $J = 1, 2, \dots, Y = 1$ ), will induce the mass splitting between the scalar and pseudoscalar components of neutral field  $\Delta^0$  of the multiplet. However, incorporating complex odd dimensional scalar multiplets in the generalized scotogenic model requires non-minimal extension [63], therefore will not be pursued here.

The scalar representation  $(J, Y) = (\frac{n}{2}, \frac{1}{2})$  with component fields is expressed as

$$\Delta_{\frac{n}{2}} = \left( \Delta_{\frac{n}{2}}^{(\frac{n+1}{2})}, \Delta_{\frac{n-2}{2}}^{(\frac{n-1}{2})}, \dots, \Delta_m^{(Q)}, \dots, \Delta_{-\frac{1}{2}}^{(0)} \equiv \frac{1}{\sqrt{2}}(S + iA), \dots, \Delta_{-m-1}^{(-Q)}, \dots, \Delta_{-\frac{n}{2}}^{(-\frac{n-1}{2})} \right)^T \quad (2.3)$$

Here the charge of the component field with  $T_3 = m$  is denoted by  $Q = m + \frac{1}{2}$ . Moreover each component of the multiplet is a complex quantity and  $(\Delta_m^{(Q)})^* = \Delta_m^{(-Q)}$ .

The neutral scalar  $S$  and pseudoscalar  $A$  component associated with  $J = n/2$  ( $n$  odd) multiplet have masses as,

$$m_S^2 = M_0^2 + \frac{1}{2} \left( \alpha + \frac{1}{4} \beta + p(-1)^{p+1} \gamma \right) v_0^2 \quad (2.4)$$

$$m_A^2 = M_0^2 + \frac{1}{2} \left( \alpha + \frac{1}{4} \beta - p(-1)^{p+1} \gamma \right) v_0^2 \quad (2.5)$$

where,  $p = \frac{1}{2}(n+1)$  that comes from  $2p \times 2p$   $C$  matrix. Moreover, because of  $Z_2$  symmetry, one can switch between  $S \rightarrow A$  or  $\gamma \rightarrow -\gamma$ . Here  $v_0$  is the Higgs VEV.

Apart from the largest charged component of the multiplet which has  $T_3 = n/2$ , the  $\gamma$  term mixes the components carrying the same amount of charge  $|Q|$ , i.e between  $\Delta_m^{(Q)}$  and

$\Delta_{-m-1}^{(Q)}$ . Therefore, the mixing matrix between components with charge  $|Q|$  is,

$$M_Q^2 = \begin{pmatrix} m_{(m)}^2 & \frac{\gamma v_0^2}{4} \sqrt{\left(\frac{n}{2} - m\right) \left(\frac{n}{2} + m + 1\right)} \\ \frac{\gamma v_0^2}{4} \sqrt{\left(\frac{n}{2} - m\right) \left(\frac{n}{2} + m + 1\right)} & m_{(-m-1)}^2 \end{pmatrix} \quad (2.6)$$

where,  $m_{(m)}^2$  is given by

$$m_{(m)}^2 = M_0^2 + \frac{1}{2} \left( \alpha - \frac{1}{2} \beta m \right) v_0^2. \quad (2.7)$$

So the mass eigenstates are,

$$\begin{aligned} \tilde{\Delta}_1^{(Q)} &= \cos \theta_Q \Delta_m^{(Q)} + \sin \theta_Q \Delta_{-m-1}^{(Q)} \\ \tilde{\Delta}_2^{(Q)} &= -\sin \theta_Q \Delta_m^{(Q)} + \cos \theta_Q \Delta_{-m-1}^{(Q)} \end{aligned} \quad (2.8)$$

with

$$\tan 2\theta_Q = \frac{2(M_Q^2)_{12}}{(M_Q^2)_{11} - (M_Q^2)_{22}} \quad (2.9)$$

Therefore the scalar multiplet can be written in terms of mass eigenstates in the following way

$$\Delta = \begin{pmatrix} \Delta^{(\frac{n+1}{2})} \\ \dots \\ \Delta_m^{(Q)} = \tilde{\Delta}_1^{(Q)} \cos \theta_Q - \tilde{\Delta}_2^{(Q)} \sin \theta_Q \\ \dots \\ \Delta^{(0)} = \frac{1}{\sqrt{2}}(S + iA) \\ \dots \\ \Delta_{-m-1}^{(-Q)} = \tilde{\Delta}_1^{(-Q)} \sin \theta_Q + \tilde{\Delta}_2^{(-Q)} \sin \theta_Q \\ \dots \end{pmatrix} \quad (2.10)$$

## 2.2 Scalar Dark Matter

Because of  $Z_2$  symmetry, one can set either  $S$  or  $A$  to be the DM candidate. In this work, we set  $S$  to be DM candidate. This consideration leads to  $|\gamma| > |\beta|/2$  and the following mass hierarchy in the components of the multiplet,

$$m_S < m_{\tilde{\Delta}_1^+} < m_{\tilde{\Delta}_1^{++}} < \dots < m_{\tilde{\Delta}_1^{(Q)}} < \dots < m_{\Delta^{(\frac{n+1}{2})}} < m_{\tilde{\Delta}_2^+} < \dots < m_{\tilde{\Delta}_2^{(Q)}} < \dots < m_A \quad (2.11)$$

For the doublet and quartet, we use the following notations

$$D = \begin{pmatrix} \Delta^+ \\ \frac{1}{\sqrt{2}}(S + iA) \end{pmatrix}, \quad \Delta = \begin{pmatrix} \Delta^{++} \\ \tilde{\Delta}_1^+ \cos \theta - \tilde{\Delta}_2^+ \sin \theta \\ \frac{1}{\sqrt{2}}(S + iA) \\ \tilde{\Delta}_1^- \sin \theta + \tilde{\Delta}_2^- \cos \theta \end{pmatrix} \quad (2.12)$$

In addition, for doublet and quartet, the Higgs-DM cubic coupling which induces the scattering of DM with nucleus in direct detection experiments, are

$$\lambda_S^d = \alpha + \frac{1}{4}\beta - \gamma, \quad \lambda_S^q = \alpha + \frac{1}{4} - 2|\gamma| \quad (2.13)$$

The theoretical constraints imposed on the doublet and the quartet couplings are given in [61].

### 3 Sommerfeld Enhancement with large Electroweak Scalar Multiplets

At present the dark matter is non-relativistic (NR) and has average velocity  $v = 220 \text{ km s}^{-1}$  in the Milky Way. In this NR limit, the exchange of massive  $W$  and  $Z$  bosons will induce Yukawa potential,  $V_Y$  and massless  $\gamma$  will induce Coulomb potential,  $V_C$  between two incoming component states of the multiplet as shown in Fig. 1 (upper and middle panels). Now if the range of the potential is larger than the characteristic Bohr radius of 2-particle state, i.e for Yukawa case,  $1/m_W \gtrsim 1/\alpha m_S$ , where  $\alpha = g^2/4\pi$ , the wavefunction of the incoming state is significantly modified inside the Yukawa potential. In other words, at NR limit, the ladder diagram as shown in Fig. 1 (lowest), is enhanced by  $\alpha m_S/m_W$  for each  $W$  boson exchange because when the mass splitting is very small compared to the mass, the intermediate  $SU(2)_L$  partner states are almost on-shell (at the threshold) and thus enhances the diagram<sup>1</sup>.

As the interaction related to annihilation or production process takes place in much shorter distance than the long range interaction responsible for the modification of the wavefunction, one can disentangle short distance physics from the long distance one. The modified 2-particle wavefunction (connected to long distance physics) is determined by solving the Schrodinger equation with an appropriate matrix-valued potential. The method of computing SE is well-studied and we have followed the prescription presented in [17, 20, 39] to compute the Sommerfeld enhanced S-wave DM DM annihilation rates  $SS \rightarrow VV$  for the large scalar multiplet of the generalized scotogenic model. In the following sections, we present the relevant parts required for the computation.

#### 3.1 The 2-particle states, potential and annihilation matrix

##### 3.1.1 The 2-particle states

The DM-DM 2-particle state,  $|SS\rangle$ , is charge neutral and CP-even state hence it only mixes with other  $Q = 0$ ,  $CP = 1$  2-particle states. Therefore, the 2-particle state vector with only charge neutral and CP even component, is given by

$$|\Phi_{\Delta_{\frac{n}{2}}}\rangle = \left( SS, AA, \Delta^{(\frac{n+1}{2})} \Delta^{(-\frac{n+1}{2})}, \dots, \tilde{\Delta}_1^{(Q)} \tilde{\Delta}_1^{(-Q)}, \tilde{\Delta}_2^{(Q)} \tilde{\Delta}_2^{(-Q)}, \dots, \right. \quad (3.1)$$

$$\left. \tilde{\Delta}_1^{(Q)} \tilde{\Delta}_2^{(-Q)}, \tilde{\Delta}_2^{(Q)} \tilde{\Delta}_1^{(-Q)}, \dots, \tilde{\Delta}_2^{(\frac{n-1}{2})} \tilde{\Delta}_1^{(-\frac{n-1}{2})} \right)^T \quad (3.2)$$

Here, the ordering of the components in the vector is arbitrary. One can adopt different ordering for convenience.

For the doublet and quartet cases, we have the 2-particle state vector as

$$\text{Doublet, } |\Phi_D\rangle = (SS, AA, \Delta^+ \Delta^-)^T \quad (3.3)$$

$$\text{Quartet, } |\Phi_\Delta\rangle = (SS, AA, \Delta^{++} \Delta^{--}, \tilde{\Delta}_1^+ \tilde{\Delta}_1^-, \tilde{\Delta}_2^+ \tilde{\Delta}_2^-, \tilde{\Delta}_1^+ \tilde{\Delta}_2^-, \tilde{\Delta}_2^+ \tilde{\Delta}_1^-)^T \quad (3.4)$$

##### 3.1.2 The Potential and Annihilation Matrix

The potential and the annihilation matrices arise from the real and imaginary part of the 2-particle state Green's function [20]. Equivalently, by integrating out the relativistic degrees of freedom, one can have effective potential and annihilation matrix in the non-relativistic limit [17, 84]. In the NR limit, the exchange of  $W$  between charged currents  $J_W^\pm$  and  $Z$  between neutral current  $J_Z$  will lead to the Yukawa potential as shown in Fig. 1. If the

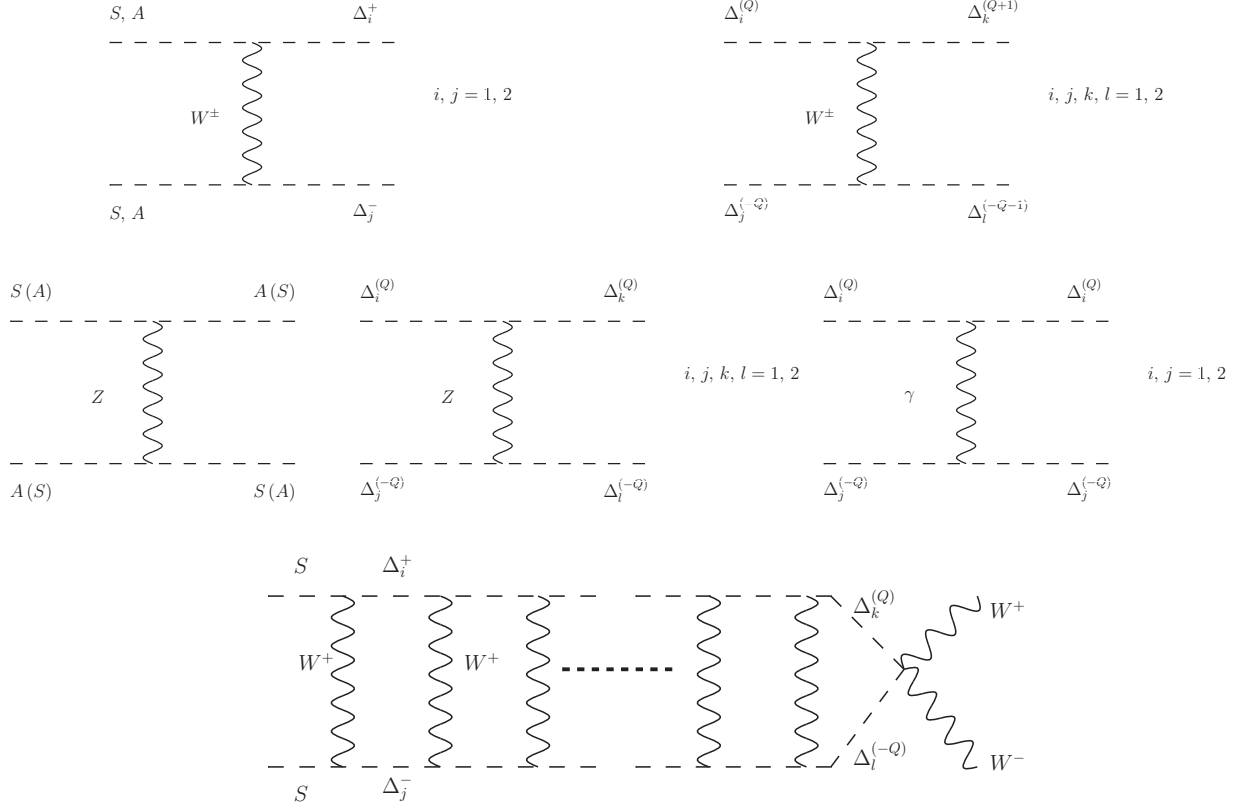


**Figure 1.** In the NR limit, the Yukawa and Coulomb potential arising from the exchange of  $W$ ,  $Z$  and  $\gamma$  (first two rows) and at third row, an example of the ladder diagram arising from the multiple exchange of  $W$  that will enhance  $SS \rightarrow WW$  cross-section. Similar ladder diagram will arise from multiple exchange of  $Z$  and  $\gamma$  and will also enhance  $SS \rightarrow WW, ZZ, \gamma\gamma, Z\gamma$ .

relative distance between two DM particles in their center of Mass (C.M.), frame is  $\vec{r}$ , the matrix element of this Yukawa potential will be of the form,

$$\langle ii' | V | jj' \rangle \equiv V_{ii',jj'} \sim \pm \frac{f_{ii',jj'} \alpha_a e^{-c_a m_W r}}{r} \quad (3.5)$$

Here,  $|ii'\rangle$  and  $|jj'\rangle$  denote the components of the 2-particle state vector given in Eq. (3.2). Also,  $f_{ii',jj'}$  is the factor that involves the combination of group theoretical values associated with  $|ii'\rangle$  and  $|jj'\rangle$  2-particle states and terms associated with the mixing between different mass eigenstates. Also,  $\alpha_a = \alpha$  and  $c_a = 1$  for  $W$  boson exchange and  $\alpha/\cos^2 \theta_W$  and  $1/\cos \theta_W$  for  $Z$  boson exchange respectively. In addition, the photon exchange between  $J_A$  currents leads to the Coulomb potential of the form  $\frac{Q^2 \alpha_{em}}{r}$ .

The S-wave annihilation of 2-particle states into two gauge bosons, is the dominant channel in the non-relativistic limit. And it can be calculated from the imaginary or the absorptive part of the 2-particle propagator  $ii' \rightarrow jj'$  as shown in Fig. 2 and is denoted by

<sup>1</sup>For an instructive presentation of various limits of momenta and masses in a Feynman diagram at the threshold region, please see [64].

$\Gamma_{ii',jj'}^{(f)}$ , where  $f$  is the final state. In the appendix we have outlined the matrix elements of both potential and S-wave annihilation matrix elements related to the scotogenic model.

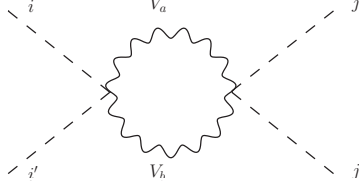


**Figure 2.** The Feynman diagram related to the S-wave annihilation matrix elements. Here,  $ii'$  and  $jj'$  takes the 2-particle state components of  $|\Phi_{\frac{n}{2}}\rangle$  and  $V_a V_b = W^+ W^-, ZZ, \gamma\gamma, \gamma Z$ .

### 3.2 Sommerfeld enhanced annihilation cross section

The radial Schrodinger matrix equation that determines the modified wavefunction in the presence of the effective potential  $V$  is

$$\frac{d^2 \Psi_{jj',ii'}}{dr^2} + \left[ \left( (m_S v)^2 - \frac{l(l+1)}{r^2} \right) \delta_{jj',kk'} - m_S V_{jj',kk'}(r) \right] \Psi_{kk',ii'} = 0 \quad (3.6)$$

where, the kinetic energy of the incoming 2-particle state  $|ii' = SS\rangle$  is,  $E = m_S v^2$ . The wavefunction  $\Psi_{jj',ii'}$  gives the transition amplitude from  $|ii'\rangle$  state to  $|jj'\rangle$  state in the presence of  $V$ . Here  $ii', jj'$  and  $kk'$  indices run over the components of the 2-particle state vector,  $|\Phi_{\Delta_{\frac{n}{2}}}\rangle$  given in Eq.(3.2).

As our focus is on the S-wave annihilation, we set  $l = 0$  and have

$$\frac{d^2 \Psi_{jj',ii'}}{dr^2} + \left[ k_{jj'}^2 \delta_{jj',kk'} + m_S \left( \frac{f_{jj',kk'} \alpha_a e^{-n_a m_W r}}{r} + \frac{Q_{kk'}^2 \alpha_{\text{em}}}{r} \delta_{jj',kk'} \right) \right] \Psi_{kk',ii'} = 0 \quad (3.7)$$

Here,  $k_{jj'}^2 = m_S(m_S v^2 - d_{jj'})$  is the momentum associated with the 2-particle state,  $|jj'\rangle$  and  $d_{jj'} = m_j + m_{j'} - 2m_S$  denotes the mass differences between DM and other states of the multiplet.  $Q_{kk'}$  is the electric charge associated with state  $|kk'\rangle$ . Also,  $\alpha_W = \alpha$  and  $n_W = 1$  for W boson exchange and  $\alpha_Z = \alpha / \cos^2 \theta_W$  and  $n_Z = 1 / \cos \theta_W$  for Z boson exchange.

Now by using dimensionless variables defined as  $x = \alpha m_S r$ ,  $\epsilon_\phi = (m_W / m_S) / \alpha$ ,  $\epsilon_v = (v/c) / \alpha$  and  $\epsilon_{d_{ii'}} = \sqrt{d_{ii'}} / m_S / \alpha$ , we re-write the coupled radial Schrodinger equations as

$$\frac{d^2 \Psi_{jj',ii'}}{dx^2} + \left[ \hat{k}_{jj'}^2 \delta_{jj',kk'} + \frac{f_{jj',kk'} n_a^2 e^{-n_a \epsilon_\phi x}}{x} + \frac{Q_{kk'}^2 \sin^2 \theta_W}{x} \delta_{jj',kk'} \right] \Psi_{kk',ii'} = 0 \quad (3.8)$$

where the dimensionless momentum,  $\hat{k}_{jj'}^2 = \epsilon_v^2 - \epsilon_{d_{jj'}}^2$ .

At very large  $x$ , the solution of Eq.(3.8) will become  $\Psi_{jj',ii'} \sim T_{jj',ii'} e^{i \hat{k}_{jj'} x}$  where  $T$  is the  $x$  independent amplitude of the wavefunction. As we have Yukawa potential in the diagonal and off-diagonal elements and Coulomb potential only in the diagonal elements of the potential, we would like to know which potential plays dominant role for the region of interest of the parameter space. It was pointed out in [20, 23, 65] that when  $e_v \lesssim e_\phi \lesssim 1$  which is the case for today's DM velocity,  $v \sim 10^{-3}$  and mass  $m_S \in (1, 30)$  TeV, the Yukawa



potential will be more dominant than the Coulomb potential and will lead to resonances through the formation of (finite numbers of) zero-energy bound states. On the other hand, if  $e_\phi \lesssim e_v \lesssim 1$ , the Coulomb potential will be more important and lead to the formation of infinite number of (quasi-continuum) zero energy bound states and hence resonance behavior will be absent [65]. Therefore as Yukawa potential is more dominant than Coulomb potential for our region of interest, in the subsequent numerical analysis, we focus on solving Eq.(3.8) with Yukawa potential only. Finally using the optical theorem as in [17], the Sommerfeld enhanced S-wave DM-DM annihilation cross section,  $SS \rightarrow f$ , is given by

$$\sigma_{SS \rightarrow f} = 2(T\Gamma^{(f)}T^\dagger)_{SS,SS} \quad (3.9)$$

where the factor 2 appears as  $|SS\rangle$  state has identical particles.

The Schrodinger equation in Eq.(3.8) is solved using MATHEMATICA with modified Variable Phase Method described in [39, 66, 67]. For highly degenerate mass spectrum, one can use the standard method described in [36, 40, 41] but when the mass-splitting becomes larger than the kinetic energy, which is the case for scotogenic model (section 4.1), some components of the matrix solution become exponentially large while taking  $x \rightarrow \infty$  and hence become numerically unstable but it can be alleviated with the above-mentioned method.

Moreover, Eq.(3.2) is written perturbatively at the zeroth order of absorptive part,  $\Gamma$  as seen in Eq.(A.3). It has been shown in [68] that such expansion will lead to the violation of perturbative unitarity due to the formation of zero energy bound state at  $v \sim 0$  and consistency requires the inclusion of the term  $i\Gamma\delta^{(3)}(\vec{r})$  in the Schrodinger equation.

## 4 Result and Discussion

In this section we have presented the numerical results and discussed their implications on the large scalar multiplets. But before doing that, we have listed the DM constraints relevant for our study. Moreover, different scalar multiplets, for example the doublet and the quartet of the scotogenic model are controlled by same parameter set of the scalar potential  $\{M, \alpha, \beta, \gamma\}$  but due to different mass spectrum, there are discernible phenomenological differences between smaller and larger multiplets. The collider constraints regarding these two multiplets is given in [55].

In this study our primary focus is on the indirect detection aspects of large scalar multiplet DM in the high mass regime ( $m_W \ll m_S$ ) because at present the DM is non-relativistic and has  $O(\text{TeV})$  mass and therefore non-perturbative Sommerfeld enhancement takes place in the DM-DM annihilation cross sections to gauge or higgs boson pair. Such enhancement takes the scalar DM of the generalized scotogenic model within the reach of H.E.S.S. [6] and future CTA [9, 10]. We will see that how the current and future experimental limits put stricter constraints on the larger scalar multiplets compared to the doublet case.

### 4.1 DM constraints and allowed parameter space

**DM relic density** The relic density of the dark matter in the universe is measured by Planck collaboration as  $\Omega_{\text{DM}}h^2 = 0.1197 \pm 0.0022$  (68% C.L.) [69]. If scalar DM of the scotogenic model is the dominant component of the DM, this relic density can be achieved either by thermal freeze-out or non-thermal process. For scalar DM, the thermal freeze-out processes are controlled by gauge and scalar interactions and proceed via the DM (co)annihilation into SM particles (for TeV scale DM, mostly into  $WW$  and  $ZZ$ ). It was shown in [28] for

doublet and [55] for quartet that, certain bounds on mass splittings between the DM and other components of the scalar multiplet are to be satisfied so that scalar DM can have the correct relic density. One can also expect Sommerfeld enhancement of the (co)annihilation processes involved in thermal freeze-out. But as shown in [19], for the freeze-out temperature,  $T_F$ , such that  $m_S/T_F \sim 20$  (the typical freeze-out condition), the SE correction is not numerically significant and it only becomes important when  $m_S/T_F \gtrsim 100$ . Moreover it has been argued in [36, 60] that the exclusion of SE in the thermal freeze out will modify the relic density at most by 30%.

Apart from thermal freeze-out process, scalar DM in the scotogenic model can be produced non-thermally through the out-of-equilibrium decay of the fermion multiplet's components (for a quick review of non-thermal DM production please see [70]). For example, in the doublet case, singlet RH neutrino can decay into  $S$  through  $N_1 \rightarrow S\nu$ . For the quartet, components of triplet fermion produce  $S$  through  $F_1^0 \rightarrow S\nu$ ,  $F_1^+ \rightarrow Sl^+$ . Here we consider the decay of lightest fermion multiplet,  $N_1$  or  $F_1$ . Fermion triplet, unlike RH neutrino, will be kept in equilibrium by gauge interactions  $F_1 F_1 \leftrightarrow VV$ . In table 1, we have listed the decoupling temperature  $T_{\text{dec}}$  below which the gauge interaction will be out of equilibrium for corresponding mass  $m_{F_1}$ . Also  $\Gamma_{F_1}^{(\text{max})}$  is the maximum decay width of  $F_1$  for  $m_{F_1}$  so that inverse decay process will never be in equilibrium. By requiring  $F$  to be decoupled from the thermal plasma, the corresponding decay width  $\Gamma_{F_1}$  and temperature  $T_D$  are given in the following table for respective mass  $m_{F_1}$ .

$m_{F_1}$	$T_{\text{dec}}$	$\Gamma_{F_1}^{(\text{max})}$	$\Gamma_{F_1}$	$T_D$
1 TeV	31.25 GeV	$10^{-12}$ GeV	$10^{-16}$ GeV	17 GeV
40 TeV	1380 GeV	$10^{-9}$ GeV	$5 \times 10^{-13}$ GeV	990 GeV

**Table 1.** Decoupling temperature for gauge interaction  $T_{\text{dec}}$ , maximum decay width  $\Gamma_{F_1}^{(\text{max})}$ , decay width  $\Gamma_{F_1}$  and temperature  $T_D$  at decay for the respective masses  $m_{F_1}$  of fermion triplet

Therefore in the case of  $T_D \lesssim T_{\text{dec}}$ , non-thermal production will also contribute to the DM content of the universe. As a result, observed DM relic density is achievable for certain ranges of  $\Gamma_{F_1}$  and  $m_S$  and the bounds on mass splittings between DM and other scalar components coming from thermal freeze-out will be relaxed to some extent. For that reason, we have focused on finding the role of the SE in present day DM annihilation rather than in the early universe. Besides the allowed range of mass splittings  $|m_i - m_S|$  are set by the constraints on Electroweak Precision observables and DM direct detection bounds as we will see in subsequent paragraphs.

**DM Direct Detection** In the scotogenic model, the elastic scattering of DM with nucleus is induced by the higgs exchange and thus controlled by the coupling  $\lambda_S$  given in Eq.(2.13). The spin independent cross section is given by,

$$\sigma_{\text{SI}} = \frac{\lambda_S^2 f^2}{4\pi} \frac{\mu^2 m_n^2}{m_h^4 m_S^2} \quad (4.1)$$

Here,  $\mu = m_n m_S / (m_n + m_S)$  is the DM-nucleon reduced mass.  $f$  parameterizes the nuclear matrix element,  $\sum_{u,d,s,c,b,t} \langle n | m_q \bar{q} q | n \rangle \equiv f m_n \bar{n} n$  and from recent lattice results [71]  $f = 0.347131$ .

The LUX 2016 [72] result has put limit on the  $m_S - \lambda_S$  plane as shown in Fig. 3 (left) and it can be seen that the direct detection experiments are reaching the sensitivity

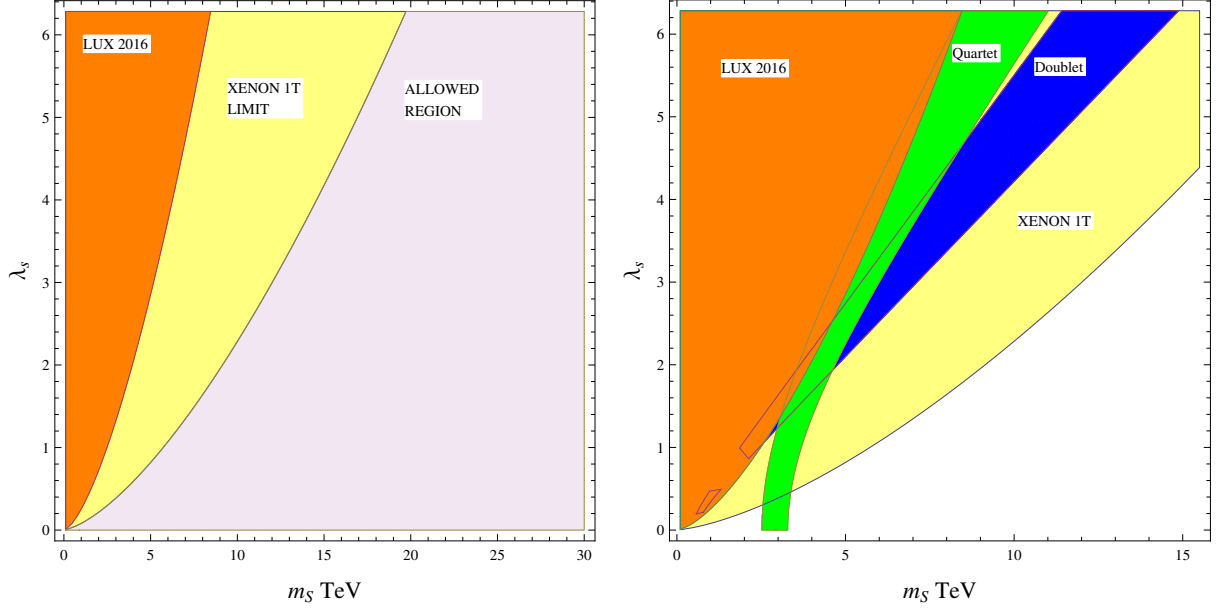


**Figure 3.** LUX(2016) exclusion limits and XENON 1T projected limits on  $m_S - \lambda_S$  plane

to probe dark matter in the high mass regime. Moreover the projected XENON 1T [73] can put stringent limit, if DM is not observed, on the  $m_S - \lambda_S$  plane and will reach the one loop corrected cross section of the order  $O(10^{-48} - 10^{-47} \text{cm}^2)$  by  $W$  and  $Z$  bosons (as shown for the doublet in [74]) even if  $\lambda_S$  is tuned to be very small.

These direct detection limits also have important implications on the thermal freeze-out process in the scotogenic model. As we can see from Fig. 3 (right) that LUX 2016 has already probed 1 – 5 TeV and 1 – 7.5 TeV region for doublet and quartet respectively. Here we have taken into account the  $O(30\%)$  modification in the relic density for not considering SE correction in freeze-out. Finally, the entire thermal freeze-out region for both doublet and quartet is enclosed by the XENON1T sensitivity limit.

**Mass splitting in the scalar multiplet** Unlike the case of the minimal DM model where the mass splitting between the DM and the charged state of the multiplet is induced radiatively after symmetry breaking and of the order  $O(100 \text{ MeV})$  [58], in the scotogenic model the mass splitting between the components of the scalar multiplet is set by the following terms in the potential,

$$V_0 \supset \beta H^\dagger \tau^a H \Delta^\dagger T^a \Delta + \gamma \left[ (H^T \epsilon \tau^a H) (\Delta^T C T^a \Delta)^\dagger + h.c \right] \quad (4.2)$$

The mass splittings among the components of the multiplet is constrained by Electroweak Precision observables (EWPO) [75–78]. They, in turn, put constraints on the allowed range for the couplings  $\beta$  and  $\gamma$ . We use the results of the EWPO for the doublet [79–82] and the quartet [61] and determine the allowed splittings. The mass splittings are defined as

$$\begin{aligned} \delta_1^d &= m_{\Delta^+} - m_S \text{ and } \delta_2^d = m_A - m_S \text{ (doublet)} \\ \delta_1^q &= m_{\Delta_1^+} - m_S, \delta_2^q = m_{\Delta^{++}} - m_S, \delta_3^q = m_{\Delta_2^+} - m_S \text{ and } \delta_4^q = m_A - m_S \text{ (quartet)} \end{aligned} \quad (4.3)$$

In addition, there is a lower bound on the mass splitting between scalar and pseudoscalar components in the scalar multiplet which arises due to the bounds on DM inelastic scattering

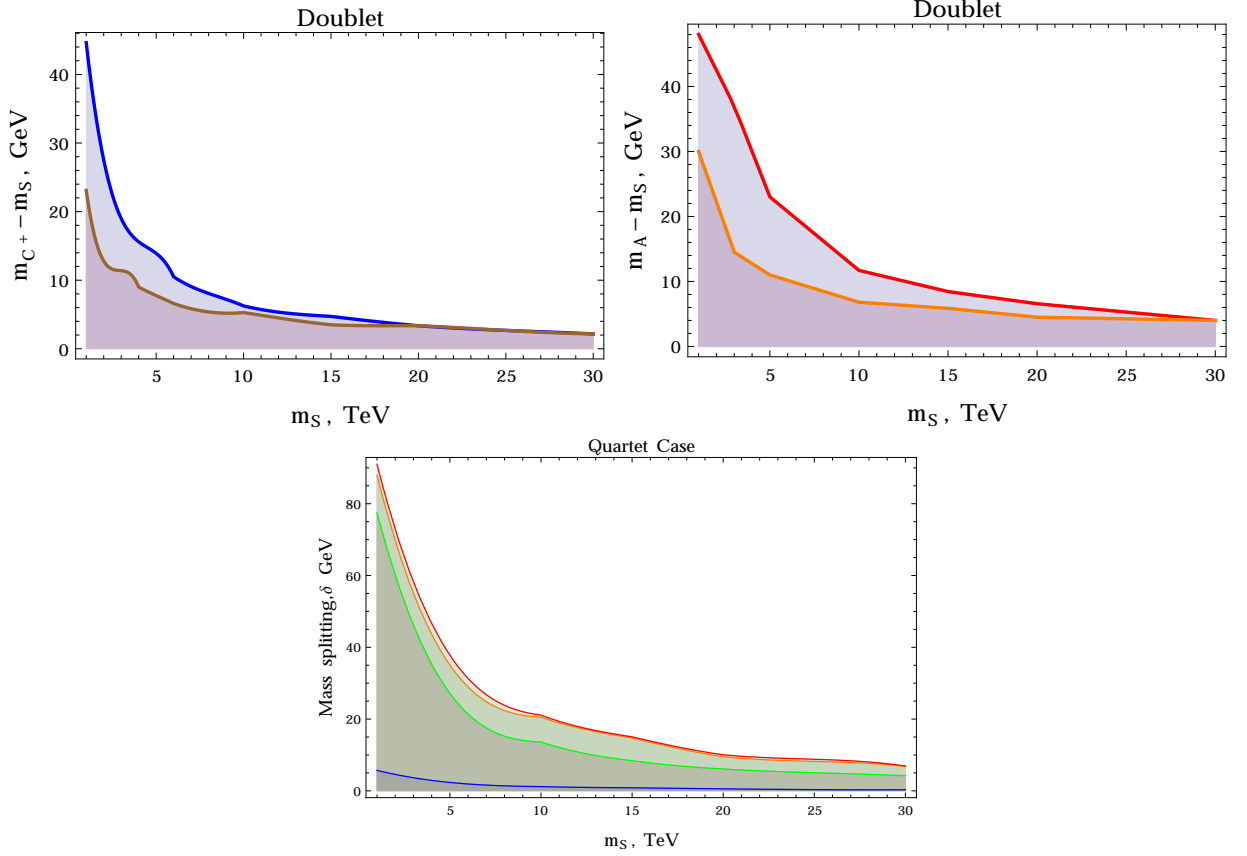


**Figure 4.** Allowed Mass splittings with DM mass,  $m_S$  in the doublet and quartet cases. In the upper left fig. allowed maximum values of  $\delta_1^d$  are marked by blue (LUX2016 result [72]) and brown (XENON1T [73]) lines. In the upper right fig. those of  $\delta_2^d$  are marked by red (LUX2016) and orange (XENON1T) lines. In the lower fig. maximum values of  $\delta_1^q, \delta_2^q, \delta_3^q$  and  $\delta_4^q$ , allowed by both LUX2016 and XENON1T, are marked by blue, green, orange and red lines respectively.

with nuclei. As the  $Z$  boson mediated inelastic scattering with nuclei is of the order of  $10^{-40} - 10^{-39} \text{ cm}^2$  and much larger than the current direct detection limits, the mass splitting between  $S$  and  $A$  has to be large enough for this scattering to be kinematically forbidden and satisfy the direct detection limits. If the velocity of DM is  $v$ , then the minimum mass splitting  $\delta_{\min}$  is

$$\delta_{\min} = \frac{m_S M_{\text{nucleus}} v^2}{2(m_S + M_{\text{nucleus}})} \quad (4.4)$$

For,  $v \sim 10^{-3}$  and  $M_{\text{nucleus}} \sim 130 \text{ GeV}$ ,  $\delta_{\min}$  ranges from  $\delta_{\min} = 57.5 \text{ keV}$  (for,  $m_S = 1 \text{ TeV}$ ) to  $\delta_{\min} \sim 65 \text{ keV}$  (for,  $m_S \gg O(\text{TeV})$ ). The allowed mass splittings for both the doublet and quartet cases are presented in Fig. 4. In passing, from Eq.(2.2) we see that  $\delta_{\min}$  for complex odd dimensional scalar multiplet with  $m_S \sim 1 \text{ TeV}$  and  $c \sim O(1)$  sets the cut off scale to be  $\Lambda \sim O(200) \text{ TeV}$  for above values of  $v$  and  $M_{\text{nucleus}}$ .

Moreover, the direct detection limits put an upper bound on  $|\lambda_S|$  and in turn constrain the allowed range of the couplings  $\beta$  and  $\gamma$  which translates into the allowed mass splittings for the scalar multiplets. As can be seen from Fig. 4 (upper panel), the LUX 2016 results and XENON1T projected limits put additional constraints on the mass splittings apart from

EWPO bounds on the doublet. On the other hand, for quartet, EWPO bounds are consistent with direct detection limits.

The mass splittings in the scalar multiplet have important impact on the Sommerfeld enhancement of the annihilation cross sections. If the mass splitting is much larger than the kinetic energy of the incoming DM particles, the almost on-shell exchange of  $SU(2)_L$  partner states in the ladder diagram which modifies the wavefunction and enhances the cross section, will be largely suppressed and for this reason, even if  $\epsilon_v \lesssim 1$  and  $\epsilon_\phi \lesssim 1$ , the SE will be negligible for annihilation cross sections.

## 4.2 Sommerfeld enhanced Cross sections

In this section we present the Sommerfeld enhanced annihilation cross sections with DM mass to various final states that are relevant for indirect detection.

### 4.2.1 $SS \rightarrow WW$

We have determined the cross sections for two cases. The first case is the (almost) degenerate limit, where the mass splittings among the components of the scalar multiplet, are set to their minimum values allowed by the constraints of section 4.1 and the second case is the maximal mass splitting limit where the mass splittings are set at their maximum allowed values. We have considered these two cases as the mass splitting is an important parameter for the SE in the scotogenic model. Also we have set the DM velocity  $v = 10^{-3}$ , which is the scale of average velocity in the galactic halo.

In Fig. 5 (left) the blue and brown lines correspond to the doublet and quartet at their (almost) degenerate limit respectively. As we can see, the cross section in the quartet case is larger than that of the doublet. The annihilation matrix elements of  $\Gamma^{(WW)}$  depends on the factor  $j^2 + j - m^2$  (appendix A.3) which increases with the isospin,  $j$  of the multiplet. Moreover, the off-diagonal potential matrix elements involve the factor  $V_{j,m}^{+2} = j^2 + j - m - m^2$  which also depends on isospin. Therefore, in case of larger multiplets, relatively large Yukawa potential and annihilation matrix elements increase the Sommerfeld corrected annihilation cross section compared to the doublet case. The first resonance peak for the doublet and the quartet has occurred at 3.1 TeV and 2 TeV respectively. There is a dip at 1.3 TeV in the quartet case though. The tree-level annihilation cross sections are marked as light blue (doublet) and green (quartet) lines.

Now we focus on the maximal mass splittings on the Sommerfeld enhanced cross sections. From Fig. 5 (left), we can see that, for doublet the resonance peak has been shifted to 14 TeV (grey; for XENON1T mass splittings) and 16 TeV (black; for LUX (2016) mass splittings). For 1 – 7 TeV range, the Sommerfeld corrected cross section is numerically comparable to the tree level cross section in the case of doublet. On the other hand, for quartet (red) the resonance peak is shifted to 3 TeV and the dip occurs at 4.2 TeV. In this case, only for 1 – 2.5 TeV range, the SE and tree-level cross sections are numerically comparable. In quartet case, from Fig. 4, we see that for the mass splitting between  $S$  and next to lightest component,  $\tilde{\Delta}_1^+$ , we have  $3.3 \gtrsim \epsilon_\delta \gtrsim 1.8$  and lead to comparable tree-level and SE cross sections. Again we have a small strip about 3.8 TeV where again tree-level and SE cross sections are comparable.

The orange and purple dashed lines in Fig. 5 (left) refer to the H.E.S.S. result and C.T.A sensitivity limits on DM annihilating into  $WW$  which we have projected on appropriate plots without carrying out any comprehensive analysis in this work. The projected limits are to be used as a reference to compare Sommerfeld enhanced cross sections of doublet and quartet.

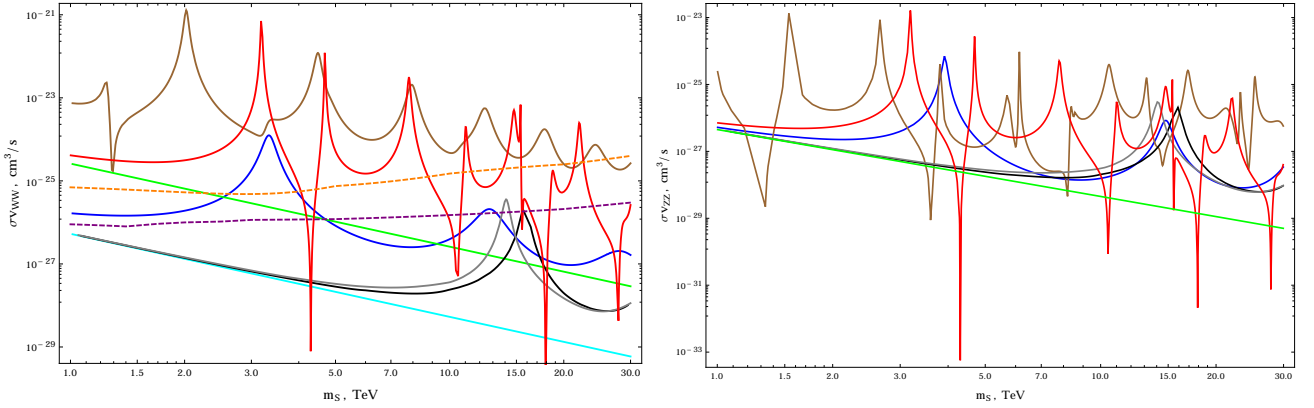


**Figure 5.** In the left fig. correlation between  $\sigma v_{WW}$  and  $m_S$ . The blue (doublet) and brown (quartet) lines represent the annihilation cross section to  $WW$  in the (almost) degenerate limit. The black (doublet, LUX2016), grey (doublet, XENON1T) and red (quartet) lines represent the cross section when mass splittings are taken as the maximum of allowed limit. The light blue (doublet) and green (quartet) lines are the tree-level annihilation cross sections. Moreover, the orange and purple dashed lines are H.E.S.S. [7] and future CTA [10] limits respectively on  $WW$  annihilation. Similarly in the right fig. correlation between  $\sigma v_{ZZ}$  and  $m_S$  for (almost) degenerate limit: blue (doublet) and brown (quartet) lines and for maximum limits of mass splittings: black (doublet, LUX2016), grey (doublet, XENON1T) and red (quartet) lines. The green line is the tree-level  $\sigma v_{ZZ}$  for both doublet and quartet.

The complete analysis will be reported elsewhere. In section 4.3 we have given qualitative explanation of resonance peaks and dips and their shifts towards smaller or larger mass.

#### 4.2.2 $SS \rightarrow ZZ$

Another important annihilation channel is the  $SS \rightarrow ZZ$ . In Fig. 5 (right), again the blue and brown lines represent the doublet and quartet  $ZZ$  annihilation in the (almost) degenerate limit. The first resonance peak for the doublet and quartet are 3.8 and 1.6 TeV respectively and the first dip occurs for quartet at 1.4 TeV. In the maximal mass splitting limit, resonance peaks occur at 14 and 16 TeV respectively for the doublet: (grey: XENON1T mass splitting) and (black: LUX2016 mass splitting) respectively. For quartet (red), the first resonance and dip occur at 3.1 and 4.2 TeV respectively. Again the mass range where the tree-level and SE cross sections are comparable, are 1 – 9 TeV for doublet and 1 – 2.5 TeV for quartet. Here, the maximum of  $SS \rightarrow ZZ$  is at the order of  $10^{-23} \text{ cm}^3 \text{ s}^{-1}$  compared to  $10^{-21} \text{ cm}^3 \text{ s}^{-1}$  of  $SS \rightarrow WW$  because in this case, the potential and annihilation matrix elements depend on the corresponding  $T_3$  eigenvalues instead of  $j$  itself like in  $WW$  case.

#### 4.2.3 $SS \rightarrow \gamma\gamma$ & $\gamma Z$

At almost degenerate limit, Fig. 6 (left) and (right) describe  $SS \rightarrow \gamma\gamma$  and  $SS \rightarrow \gamma Z$  respectively for doublet (orange) and quartet (blue). The occurrence of the resonances and dips in both processes are almost the same. The only difference is that for  $SS \rightarrow \gamma\gamma$  the maximum peaks are of the order of  $10^{-25} \text{ cm}^3 \text{ s}^{-1}$  (doublet) and  $10^{-24} \text{ cm}^3 \text{ s}^{-1}$  (quartet). On the other hand, for  $SS \rightarrow \gamma Z$ , the maximum peaks are of the order  $10^{-24} \text{ cm}^3 \text{ s}^{-1}$  (doublet) and  $10^{-22} \text{ cm}^3 \text{ s}^{-1}$  (quartet).

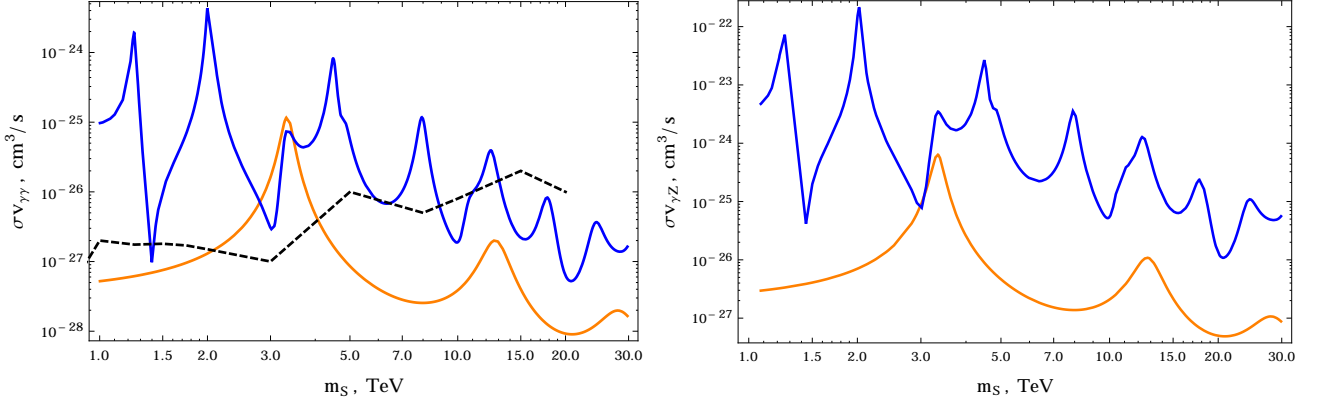


**Figure 6.** Correlation of  $\sigma v_{\gamma\gamma}$  (left fig.) and  $\sigma v_{\gamma Z}$  (right fig.) with  $m_S$  for the doublet (orange line) and quartet (blue line) cases at the almost degenerate limits. Also the black dashed line in left fig is the H.E.S.S. limits on  $\gamma\gamma$  annihilation [8].

When the mass splittings are taken to be their maximum allowed limits, both  $SS \rightarrow \gamma\gamma$  and  $SS \rightarrow \gamma Z$  are greatly suppressed because large mass splittings don't allow the intermediate charged state to be on-shell (as the momentum becomes imaginary for  $v \sim 10^{-3}$ ) in the ladder diagram and thus  $T_{SS, \tilde{\Delta}_i^{(Q)} \tilde{\Delta}_i^{(-Q)}}$  factors that enter in the cross-section for  $SS \rightarrow \gamma\gamma$  are effectively zero. Similar arguments also hold for  $SS \rightarrow \gamma Z$  case.

Consequently, in such limit both processes can be induced by one-loop contribution of charged states. For the mass range of 1 – 30 TeV, in case of  $SS \rightarrow \gamma\gamma$ , the cross sections are of the order,  $10^{-28} - 10^{-31} \text{ cm}^3\text{s}^{-1}$  (both doublet and quartet) and in case of  $SS \rightarrow \gamma Z$ , they are of the order,  $10^{-29} - 10^{-32} \text{ cm}^3\text{s}^{-1}$  (doublet) and  $10^{-27} - 10^{-30} \text{ cm}^3\text{s}^{-1}$  (quartet).

### 4.3 Discussion

In section 4.2 we have seen the shift of resonance peaks with increasing mass splitting and the occurrence of dips for the quartet case which was absent in the doublet case. Here we have used a two state system with finite square well potential to illustrate these features in a simple way.

The particle state is given by  $|\chi\rangle = (\chi_1, \chi_2)$  and  $\chi_1$  is considered to be DM state. If the 2-particle state vector is  $|\Psi\rangle = (\chi_1\chi_1, \chi_2\chi_2)$ , the square-well potential in this basis is

$$V = \begin{pmatrix} 0 & -|V_{12}| \\ -|V_{12}| & -|V_{22}| \end{pmatrix} \theta(L - r) + \begin{pmatrix} 0 & 0 \\ 0 & 2\delta \end{pmatrix}$$

where,  $L$  is the range of the potential. Moreover, the mass splitting is,  $\delta = m_{\chi_2} - m_{\chi_1}$ . The eigenvalues giving attractive and repulsive potential energy and the corresponding eigenstates are

$$\lambda_{\pm} = \frac{1}{2} \left( -|V_{22}| + 2\delta \pm \sqrt{(|V_{22}| - 2\delta)^2 + 4V_{12}^2} \right) \text{ and } |\lambda_{\pm}\rangle = \begin{pmatrix} \frac{\lambda_{\mp}}{V_{12} \sqrt{1 + \frac{\lambda_{\mp}^2}{V_{12}^2}}} \\ \frac{1}{\sqrt{1 + \frac{\lambda_{\mp}^2}{V_{12}^2}}} \end{pmatrix} \quad (4.5)$$



The transition amplitude from  $|\lambda_a\rangle$  state inside the potential well to  $|i\rangle$  state outside the region of the potential, is given by

$$T_{ai} = \frac{1}{\cos(k_{\text{in},a}L) - i \frac{k_{\text{out},i}}{k_{\text{in},a}} \sin(k_{\text{in},a}L)} \quad (4.6)$$

where,  $k_{\text{in},a} = \sqrt{m_{\chi_1}(m_{\chi_1}v^2 - \lambda_a)}$  with  $a = +, -$ , denotes the momentum inside the potential for  $|\lambda_{\pm}\rangle$  states. And  $k_{\text{out},1} = m_{\chi_1}v$  and  $k_{\text{out},2} = \sqrt{m_{\chi_1}(m_{\chi_1}v^2 - 2\delta)}$  denote the momentum associated with  $|\chi_1\chi_1\rangle$  and  $|\chi_2\chi_2\rangle$  states respectively in the outside region of the potential.

**1.  $|\mathbf{V}_{12}| \gg |\mathbf{V}_{22}|$ ,  $\delta$  limit** In this limit, we have the eigenvalues,

$$\lambda_+ \sim |V_{12}| - \frac{1}{2}|V_{22}| + \delta, \quad \lambda_- \sim -|V_{12}| - \frac{1}{2}|V_{22}| + \delta \quad (4.7)$$

and the eigenstates and the transformation matrix are,

$$|\lambda_+\rangle = \begin{pmatrix} c_{1+} \\ c_{2+} \end{pmatrix}, \quad |\lambda_-\rangle = \begin{pmatrix} c_{1-} \\ c_{2-} \end{pmatrix}, \quad U_{ia} = \begin{pmatrix} c_{1+} & c_{1-} \\ c_{2+} & c_{2-} \end{pmatrix} \quad (4.8)$$

Here, the matrix elements  $c_{ia}$  are,

$$\begin{aligned} c_{1+} &\sim \frac{1}{\sqrt{2}} \left( -1 - \frac{|V_{22}|}{4|V_{12}|} + \frac{\delta}{2|V_{12}|} \right), \quad c_{1-} \sim \frac{1}{\sqrt{2}} \left( 1 - \frac{|V_{22}|}{4|V_{12}|} + \frac{\delta}{2|V_{12}|} \right) \\ c_{2+} &\sim \frac{1}{\sqrt{2}} \left( 1 - \frac{|V_{22}|}{4|V_{12}|} + \frac{\delta}{2|V_{12}|} \right), \quad c_{2-} \sim \frac{1}{\sqrt{2}} \left( + - \frac{|V_{22}|}{4|V_{12}|} - \frac{\delta}{2|V_{12}|} \right) \end{aligned} \quad (4.9)$$

The transition amplitudes  $T_{ai}$  in the limit,  $v \rightarrow 0$ <sup>2</sup>, are

$$T_{+i} \sim \left[ \cosh \left( \sqrt{m_{\chi_1}|V_{12}|}L \left( 1 + \frac{\delta}{2|V_{12}|} - \frac{|V_{22}|}{4|V_{12}|} \right) \right) + \sqrt{\frac{2\delta_i}{|V_{12}|}} \sinh \left( \sqrt{m_{\chi_1}|V_{12}|}L \left( 1 + \frac{\delta}{2|V_{12}|} - \frac{|V_{22}|}{4|V_{12}|} \right) \right) \right]^{-1} \quad (4.10)$$

$$T_{-i} \sim \left[ \cos \left( \sqrt{m_{\chi_1}|V_{12}|}L \left( 1 - \frac{\delta}{2|V_{12}|} + \frac{|V_{22}|}{4|V_{12}|} \right) \right) - \sqrt{\frac{2\delta_i}{|V_{12}|}} \sin \left( \sqrt{m_{\chi_1}|V_{12}|}L \left( 1 - \frac{\delta}{2|V_{12}|} + \frac{|V_{22}|}{4|V_{12}|} \right) \right) \right]^{-1} \quad (4.11)$$

where,  $\delta_1 = 0$  and  $\delta_2 = \delta$ .

Now the transmission amplitude,  $d_{ij}$  in the  $|\chi_i\chi_i\rangle$  basis is,

$$d_{ij} = U_{ia}T_{aj} \quad (4.12)$$

And if the annihilation matrix  $\Gamma^{(VV)}$  is taken as,

$$\Gamma^{(VV)} = \frac{\pi\alpha^2}{m_{\chi_1}^2} \begin{pmatrix} 1 & 1 \\ 1 & 1 \end{pmatrix} \quad (4.13)$$

---

<sup>2</sup>we take this limit to simplify the expressions further.



the Sommerfeld enhanced cross section for  $\chi_1\chi_1 \rightarrow VV$  is,

$$\sigma_{11} = (d\Gamma d^\dagger)_{11} = \frac{\pi\alpha^2}{m_{\chi_1}^2} (|d_{11}|^2 + 2\text{Re}(d_{11}^*d_{12}) + |d_{12}|^2) \quad (4.14)$$

where,  $d_{11} = c_{1+}T_{+1} + c_{1-}T_{-1}$  and  $d_{12} = c_{1+}T_{+2} + c_{1-}T_{-2}$ .

Here,  $T_{+1}$  and  $T_{+2}$  are exponentially suppressed because of repulsive potential  $\lambda_+$ . Moreover, the presence of small mass splitting  $\delta$  reduces the attractive potential energy in  $\lambda_-$ . For simplicity, in the limit  $\delta/|V_{12}|$ ,  $|V_{22}|/|V_{12}| \ll 1$ , the resonance in  $T_{-1}$  and  $T_{-2}$  would occur in

$$\sqrt{m_{\chi_1}|V_{12}|}L = \frac{(2n-1)\pi}{2}, \quad n = 1, 2, \dots$$

In addition, non-zero small  $\delta$  ( $|V_{22}|$ ) shifts the resonance to larger (smaller)  $m_{\chi_1}$ . Fig. 7 (upper left) presents this behavior.

**2.  $|V_{22}| \gg |V_{12}|$ ,  $\delta$  limit** In this limit, the eigenvalues are

$$\lambda_+ \sim \frac{|V_{12}|^2}{2|V_{22}|} \left(1 + \frac{2\delta}{|V_{22}|}\right), \quad \lambda_- \sim -|V_{22}| - \frac{|V_{12}|^2}{|V_{22}|} + 2\delta \quad (4.15)$$

And the components  $c_{ia}$  of the eigenvectors are,

$$\begin{aligned} c_{+1} &\sim -1 + O(|V_{12}|^2/|V_{22}|^2) + O(4\delta^2/|V_{22}|^2), \quad c_{-1} \sim \frac{|V_{12}|}{|V_{22}|} + \frac{2|V_{12}|\delta}{|V_{22}|^2} \\ c_{+2} &\sim \frac{|V_{12}|}{|V_{22}|} + \frac{2|V_{12}|\delta}{|V_{22}|^2}, \quad c_{-2} \sim 1 + O(|V_{12}|^2/|V_{22}|^2) + O(4\delta^2/|V_{22}|^2) \end{aligned} \quad (4.16)$$

For the second case, the amplitudes are,

$$T_{+i} \sim \left[ \cosh\left(\sqrt{m_{\chi_1}\lambda_+}L\right) + \sqrt{\frac{2\delta_i}{\lambda_+}} \sinh\left(\sqrt{m_{\chi_1}\lambda_+}L\right) \right]^{-1} \quad (4.17)$$

$$\begin{aligned} T_{-i} &\sim \left[ \cos\left(\sqrt{m_{\chi_1}|V_{22}|}L\left(1 - \frac{\delta}{|V_{22}|} + \frac{|V_{12}|^2}{2|V_{22}|^2}\right)\right) - \sqrt{\frac{2\delta_i}{|V_{22}|}} \right. \\ &\quad \left. \sin\left(\sqrt{m_{\chi_1}|V_{22}|}L\left(1 - \frac{\delta}{|V_{22}|} + \frac{|V_{12}|^2}{2|V_{22}|^2}\right)\right) \right]^{-1} \end{aligned} \quad (4.18)$$

Here,  $T_{+i}$  will be suppressed with large  $m_{\chi_1}$  and  $T_{-i}$  will have resonances for certain values of  $m_{\chi_1}$ . But compared with the first case Eq.(4.10),  $T_{+i}$  in Eq.(4.17) will be less suppressed with  $m_{\chi_1}$  because  $\lambda_+$  for the second case Eq.(4.15) is much smaller than that of the first case Eq.(4.7). The  $d_{11}$  and  $d_{12}$  are

$$d_{11} = c_{+1}T_{+1} + c_{-1}T_{-1}, \quad d_{12} = c_{+1}T_{+2} + c_{-1}T_{-2} \quad (4.19)$$

As  $|c_{+1}| \sim 1$  and  $T_{+1}$  is not as suppressed as the first case, for small  $m_{\chi_1}$ , both terms will contribute to the  $|d_{11}|$  and cancellation between positive  $|c_{\pm 1}T_{\pm 1}|^2$  terms and the interference term  $2\text{Re}(c_{+1}^*T_{+1}^*c_{-1}T_{-1})$  for particular values of  $m_{\chi_1}$  leads to the resonance dips in  $|d_{11}|$ . For very large  $m_{\chi_1}$ ,  $T_{+1}$  will be infinitesimal, hence  $d_{11} \sim c_{-1}T_{-1}$  and no dips will occur in  $|d_{11}|$ . Similar reasoning also holds for dips in  $|d_{12}|$ . Fig. 7 (upper right) represents this behavior.

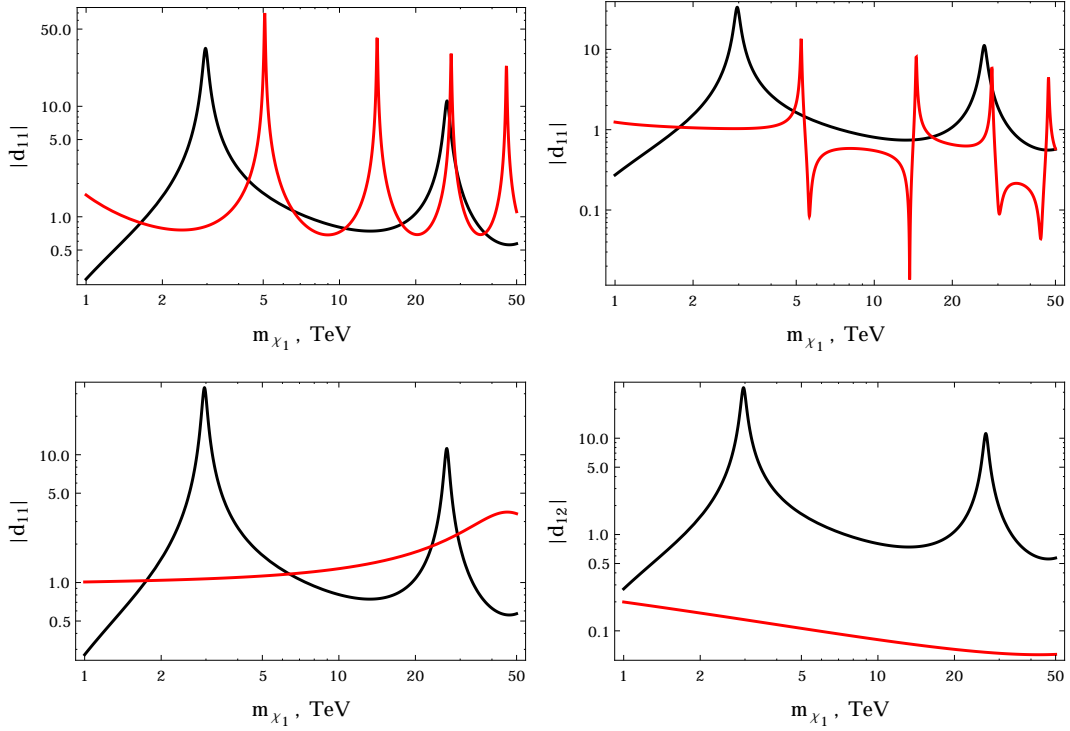


**Figure 7.**  $|d_{11}|$  and  $|d_{12}|$  with respect to  $m_{\chi_1}$  in three cases and in all figures black line corresponds to  $|V_{12}| = \sqrt{2}\alpha m_W$ ,  $|V_{22}| = \alpha m_W$ ,  $\delta = 0$ . Red line corresponds to in upper left fig.  $|V_{12}| = 10\alpha m_W$ ,  $|V_{22}| = \alpha m_W$ ,  $\delta = 0$ , upper right fig.  $|V_{12}| = \sqrt{2}\alpha m_W$ ,  $|V_{22}| = 10\alpha m_W$ ,  $\delta = 0$ .  $|d_{12}|$  is similar so it is not shown for these two cases. In lower left and right fig. red line corresponds to  $|d_{11}|$  and  $|d_{12}|$  respectively for  $|V_{12}| = \sqrt{2}\alpha m_W$ ,  $|V_{22}| = \alpha m_W$ ,  $\delta = 50$  GeV.

**3.  $\delta \gg |\mathbf{V}_{12}|, |\mathbf{V}_{22}|$  limit** Finally, we consider the limit  $\delta \gg |\mathbf{V}_{12}|, |\mathbf{V}_{22}|$ . In the zero energy limit, as the mass difference is larger than the kinetic energy of DM state, the transition to  $|\chi_2\chi_2\rangle$  is not kinematically possible and thus the cross section is not enhanced.

In this limit, the eigenvalues are,

$$\lambda_+ \sim 2\delta - |V_{22}| + \frac{|V_{12}|^2}{2\delta}, \quad \lambda_- \sim -\frac{|V_{12}|^2}{2\delta} \quad (4.20)$$

Here,  $\lambda_+ \gg |\lambda_-|$ . And the components of the eigenvectors are

$$\begin{aligned} c_{1+} &\sim -\frac{|V_{12}|}{2\delta}, \quad c_{1-} \sim 1 \\ c_{2+} &\sim 1, \quad c_{2-} \sim \frac{|V_{12}|}{2\delta} \end{aligned} \quad (4.21)$$

In this limit, the amplitudes  $T_{ai}$  are,

$$T_{+i} \sim \left[ \cosh(\sqrt{m_{\chi_1}\lambda_+}L) + \sqrt{\frac{2\delta_i}{\lambda_+}} \sinh(\sqrt{m_{\chi_1}\lambda_+}L) \right]^{-1} \quad (4.22)$$

$$T_{-i} \sim \left[ \cos(\sqrt{m_{\chi_1}|\lambda_-|}L) - \sqrt{\frac{2\delta_i}{|\lambda_-|}} \sin(\sqrt{m_{\chi_1}|\lambda_-|}L) \right]^{-1} \quad (4.23)$$

Here,  $T_{+1}$  and  $T_{+2}$  will be again exponentially suppressed as the first case. So  $d_{11} \sim c_{1-}T_{-1}$  and  $d_{12} \sim c_{1-}T_{-2}$ . In the  $v \rightarrow 0$  limit, for  $\delta \gg |V_{12}|$  such that,  $|\lambda_-| \sim 0$ , then  $T_{-1} \sim 1$  and  $T_{-2}$  scales as  $T_{-2} \sim 1/\sqrt{m_{\chi_1}}$  and hence it is negligible for  $O(\text{TeV})$  mass. So for very large mass splittings there won't be any enhancement in the cross section.

On the other hand, if  $\delta \gtrsim |V_{12}|$  and  $|\lambda_-|$  is small but non-zero, at certain large mass  $m_{\chi_1}$  so that  $\sqrt{m_{\chi_1}}|\lambda_-|L \sim \pi/2$ , the resonance condition is fulfilled in  $T_{-i}$  and we would again see resonance in the annihilation cross section which is non-observable in the smaller mass range. In Fig. 7 (lower left and right) we can see these behavior in  $d_{11}$  and  $d_{12}$  respectively.

These simplified results for the square-well can be inferred for larger electroweak multiplets with short-ranged potential such as Yukawa potential. For larger representations, large group theoretic factors  $f_{ab}$  associated with  $SU(2)$  ladder operators enter as the coefficients of Yukawa potential, as in Eq.(3.7) and such large coefficients lead to large matrix elements  $|V_{ab}|$ . From the above three limits, we may encounter the following cases,

1. If the DM 2-particle state is denoted by  $|1\rangle \equiv |\chi_1\chi_1\rangle$  state and  $|a \neq 1\rangle$  as other charged and pseudoscalar 2-particle states  $|\chi_i\chi_j\rangle$ , any or more than one matrix elements  $|V_{1a}|$  ( $a = 1, \dots, N$ ) of  $N \times N$  potential matrix, satisfy  $|V_{1a}| \gg |V_{bc}|, \delta_a$ , where,  $b, c \neq 1$  and  $\delta_a = m_j + m_k - 2m_1$  for  $|a = \chi_j\chi_k\rangle$  state,  $|1\rangle$  will have larger overlapping with the attractive states  $|\lambda_- \rangle$ 's (as  $c_{1-} \sim 1/\sqrt{2}$ ) and  $d_{1a}$  will have resonances for certain  $m_{\chi_1}$  and hence the annihilation cross section  $\chi_1\chi_1 \rightarrow f$  will be enhanced. Moreover, non-zero mass splitting shifts the resonance peaks to larger mass value. We have seen these features in the doublet case in Fig. 5 and 6.
2. In contrast, when  $|V_{bc}| \gg |V_{1a}|, \delta_a$ , where  $b, c \neq 1$ ,  $|1\rangle$  will have smaller overlapping with attractive states (as  $c_{1-} \sim |V_{1a}|/|V_{bc}|$ ) and along with resonances, there will be resonance dips for certain  $m_{\chi_1}$  values as seen for  $2 \times 2$  square-well potential case. We have seen the appearance of dips for the quartet case in Fig. 5 and 6.
3. Finally, for  $\delta_a \gg |V_{bc}|$ , where  $|a \equiv \chi_j\chi_k\rangle$  and  $j, k \neq 1$ , the channel  $\chi_1\chi_1 \rightarrow \chi_j\chi_k$  will be kinematically closed and will not contribute to the enhancement of the annihilation cross section. This was the case of  $\gamma\gamma$  and  $\gamma Z$  annihilation with large mass splittings.

## 5 Conclusion and outlook

In this study we have demonstrated that the Sommerfeld enhancement of the DM annihilation cross section increases with the size of the multiplet but in the case of larger multiplet resonance dips or suppression for certain values of the DM mass appear along with resonances. In the multi-channel case, for larger multiplet, not only the number of potential matrix elements  $V_{SS,jj'}, jj' = SS, \dots, \tilde{\Delta}_j^+ \tilde{\Delta}_{j'}^-$  is large than that of smaller multiplet but also the matrix elements are comparatively larger due to factors related to  $SU(2)_L$  raising operator. As we have investigated the region where Yukawa potential has dominated over Coulomb potential, our case resembles the first case of square well example given in section 4.3.

In addition, the dips occur in the multi-channel because of large potential matrix elements  $V_{ii',jj'}, ii', jj' \neq SS$  which not only decrease the overlapping of the  $|SS\rangle$  states on attractive eigenstates of the potential, which are responsible for the enhancement but also induce destructive interference in transition amplitudes  $T_{SS,jj'}, jj' = SS, \dots, \tilde{\Delta}_j^+ \tilde{\Delta}_{j'}^-$  which enter into the cross section Eq.(3.9). This case resembles the second case of square well

example in section 4.3. Besides we can see that the dip can occur for short ranged potential in multi channel process, whereas it was attributed to Coulomb interaction in [83].

Moreover, when mass splittings are taken as their maximum allowed limit, we can see from Fig. 5 (left) that for doublet, the tree-level and Sommerfeld enhanced cross sections are comparable for 1 – 7 TeV mass range whereas only for 1 – 2.5 TeV (outside the thermal DM region), one has comparable tree-level and SE cross-section of  $SS \rightarrow WW$ . Still there is a small strip about 3.8 TeV, one again has the comparable tree-level and SE cross section. Apart from 10, 17 and 28 TeV, SE cross section is larger than the tree-level cross section of  $SS \rightarrow WW$ . Comparatively larger SE is observed for the quartet, is due to the small mass splitting between DM and next to lightest single charged component allowed by EWPO, for which  $\epsilon_{d_{\tilde{\Delta}_1^+ \tilde{\Delta}_1^-}} \lesssim 1$  except for few small mass ranges. Similar pattern is also seen in Fig. 5 (right) for  $SS \rightarrow ZZ$  cross section.

Consequently large Sommerfeld enhanced DM annihilation cross section have important implications on the indirect detection. Without undertaking the comprehensive analysis for the scotogenic model, we have only projected the exclusion limits of H.E.S.S. [7] and the future sensitivity limit of CTA [10] of annihilation cross section to  $WW$  on our  $SS \rightarrow WW$  cross section plot and exclusion limits of H.E.S.S. [8] of  $\gamma\gamma$  annihilation on our  $SS \rightarrow \gamma\gamma$  plot so that we can see how far the experimental sensitivity has been reached to probe the indirect detection signals for the Scotogenic model with different sizes of scalar multiplets. It can be seen from Fig. 5 (left) that H.E.S.S. has already achieved the sensitivity to probe the entire 1 – 30 TeV mass range for the quartet except  $m_S \sim 27$  TeV for the (almost) degenerate limit and dips at certain mass values for the allowed maximum mass splitting. On the other hand, for the doublet, except for 2.5 – 4 TeV for (almost) degenerate limit and almost all of 1 – 30 TeV for allowed maximum limit, are below the H.E.S.S. limit. Future CTA sensitivity limit is improved by  $O(10)$  compared to H.E.S.S. limits.

For  $SS \rightarrow \gamma\gamma, \gamma Z$  cases, the Sommerfeld enhanced cross section is obtained only for (almost) degenerate limit because maximum allowed mass splitting suppress the  $T_{SS,jj}, jj = \tilde{\Delta}_j^{(Q)} \tilde{\Delta}_j^{(-Q)}$  factors and thus annihilation becomes negligible. For such case, the  $\gamma\gamma$  and  $\gamma Z$  annihilation proceed through one loop process via charged scalars exchange and has  $10^{-32} - 10^{-27} \text{ cm}^2 \text{ s}^{-1}$  for doublet and quartet. From Fig. 6 (left), we can see that H.E.S.S. limit can already probe 1 – 9 (except for dip at 1.4 TeV) and 11.5 – 14 TeV of their considered 1 – 20 TeV mass range for the quartet whereas for the doublet only 2.1 – 4.1 TeV out of 1 – 20 TeV is within the reach of H.E.S.S.

From the present investigation we can infer that in scotogenic model, the Sommerfeld enhanced cross sections of higher scalar multiplet will be larger than the doublet. Although the projection of H.E.S.S. and future CTA sensitivity limits on  $SS \rightarrow WW$  and  $SS \rightarrow \gamma\gamma$  plots have already given us the order of magnitude prospects to detect the indirect signal of DM annihilation with larger multiplets, a detailed gamma-ray spectral analysis that includes specific features (as in the case for doublet [60, 85]) as well as the contribution from P-wave annihilation, specially in S-wave suppressed (occurrence of dips) cases [86], are needed to be carried out for determining the viability of larger multiplets [87]. Nevertheless, the DM of higher scalar multiplet is more likely to be found in the current and future indirect detection experiments because of their large Sommerfeld enhanced annihilation cross sections.

## Note Added

During the preparation of this manuscript, [88] has appeared which investigated the scalar DM relic density of  $j = 5/2$  and  $j = 7/2$  multiplets in the high mass regime but didn't include the prospect of detecting indirect signals in current H.E.S.S. or future CTA experiments.

## Acknowledgements

We would like to thank Xiaoyong Chu and Camilo Garcia-Cely for stimulating remarks and critical reading of the manuscript. T.A.C. is indebted to Fabrizio Nesti and Goran Senjanović for pointing out the role of higher dimensional operator in mass splittings of complex odd dimensional scalar multiplets and also would like to thank Mahbub Majumdar and Arshad Momen for discussion.

## A The Potential and Annihilation Matrix Elements

In this appendix we have made an inventory the NR limit of the component fields and the interaction part of the NR action that gives the potential and the S-wave annihilation matrix for the generalized scotogenic model. Our calculation closely followed the methods given in [17, 84].

### A.1 NR Limit

In the NR limit, the component fields are

$$\begin{aligned} S(A)(x) &= \frac{1}{\sqrt{2m_{S(A)}}} \left( \zeta_{S(A)}(\vec{x}, t) e^{-im_{S(A)}t} + \zeta_{S(A)}^*(\vec{x}, t) e^{-im_{S(A)}t} \right) \\ \tilde{\Delta}_i^{(Q)}(x) &= \frac{1}{\sqrt{2m_{\tilde{\Delta}_i^{(Q)}}}} \left( \xi_{\tilde{\Delta}_i^{(Q)}}(\vec{x}, t) e^{-im_{\tilde{\Delta}_i^{(Q)}}t} + \eta_{\tilde{\Delta}_i^{(-Q)}}^*(\vec{x}, t) e^{-im_{\tilde{\Delta}_i^{(Q)}}t} \right) \end{aligned} \quad (\text{A.1})$$

Here,  $\zeta_{S(A)}$  and  $\zeta_{S(A)}^*$  are associated with the annihilation and creation of  $S(A)$  fields.  $\xi_{\tilde{\Delta}_i^{(Q)}}$  and  $\eta_{\tilde{\Delta}_i^{(-Q)}}^*$  corresponds to annihilation of  $\tilde{\Delta}_i^{(Q)}$  and creation of  $\tilde{\Delta}_i^{(-Q)}$  respectively and vice versa. At  $O(\text{TeV})$  range, the allowed mass splittings between DM component and other components of the multiplet as mentioned in section 4, is small compared to the mass itself. So in the subsequent analysis, we set,  $m_i \sim m_S$  in Eq.(A.1) of the component fields. Moreover the annihilation and creation of 2-particle states  $|SS\rangle$  or  $|AA\rangle$  correspond to  $\zeta_i \zeta_i$  and  $\zeta_i^* \zeta_i^*$  respectively. Similarly those of the state  $|\tilde{\Delta}_i^{(Q)} \tilde{\Delta}_j^{(-Q)}\rangle$  correspond to  $\xi_{\tilde{\Delta}_i^{(Q)}} \eta_{\tilde{\Delta}_j^{(-Q)}}^*$  and  $\xi_{\tilde{\Delta}_i^{(Q)}}^* \eta_{\tilde{\Delta}_j^{(-Q)}}^*$  respectively.

In addition, at fixed time  $x^0$ , the corresponding the 2-particle fields, which are the components of the 2-particle field vector  $\Phi(x, \vec{r})$ , are defined as

$$\begin{aligned} \Phi_{ii'}^N(x, \vec{r}) &= \frac{1}{\sqrt{2}} \zeta_i(\vec{x} - \vec{r}/2, x^0) \zeta_i(\vec{x} + \vec{r}/2, x^0) \quad i, i' = S, A \\ \Phi_{ii'}^C(x, \vec{r}) &= \xi_i(\vec{x} - \vec{r}/2, x^0) \eta_i(\vec{x} + \vec{r}/2, x^0) \quad i = \tilde{\Delta}_i^{(Q)}, i' = \tilde{\Delta}_i^{(-Q)} \end{aligned} \quad (\text{A.2})$$

where  $x$  is the center of mass coordinate for 2-particle system and  $\vec{r}$  represents the relative separation between them. Also  $1/\sqrt{2}$  is due to identical particles. The NR effective action

for 2-particle fields is now defined as

$$S_{\text{eff}} = \int d^4x d^3r \Phi^\dagger(x, \vec{r}) \left( i\partial_{x^0} + \frac{\nabla_x^2}{4m_S} + \frac{\nabla_r^2}{m_S} - V(\vec{r}) + 2i\Gamma\delta^{(3)}(\vec{r}) \right) \Phi(x, \vec{r}) \quad (\text{A.3})$$

## A.2 The Potential Matrix elements

The potential matrix induced by the exchange of the gauge bosons can be derived from the gauge current interaction of the Lagrangian,

$$\mathcal{L} \supset J_\mu^+ W^{+\mu} + J_\mu^- W^\mu + J_\mu^Z Z^\mu + J_\mu^A A^\mu \quad (\text{A.4})$$

After integrating out the light or relativistic degrees of freedom i.e gauge bosons, these terms induce the current current interactions in the effective action of the following form,

$$S_{\text{eff}} \supset - \int \frac{d^4x d^3y}{8\pi r} (2J_0^+(x)J_0^-(x^0, \vec{y})e^{-m_W r} + J_0^Z(x)J_0^Z(x^0, \vec{y})e^{-m_Z r} + J_0^A(x)J_0^A(x^0, \vec{y})) \quad (\text{A.5})$$

where  $r = |\vec{x} - \vec{y}|$ . Also for non-relativistic current,  $J_0 \gg J_i$ .

**Matrix elements due to Z and  $\gamma$  exchange** The part of the neutral current containing the charged component fields with  $Q$  is

$$J_0^Z \supset \frac{ig}{\cos\theta_W} \left( z_{11}\tilde{\Delta}_1^{(-Q)}\overleftrightarrow{\partial}_0\tilde{\Delta}_1^{(Q)} + z_{22}\tilde{\Delta}_2^{(-Q)}\overleftrightarrow{\partial}_0\tilde{\Delta}_2^{(Q)} + z_{12}(\tilde{\Delta}_1^{(-Q)}\overleftrightarrow{\partial}_0\tilde{\Delta}_2^{(Q)} + \tilde{\Delta}_2^{(-Q)}\overleftrightarrow{\partial}_0\tilde{\Delta}_1^{(Q)}) \right) \quad (\text{A.6})$$

Here the factors  $z_{ij}$  are

$$\begin{aligned} z_{11} &= (m - Q \sin^2 \theta_W) \cos^2 \theta_Q + (m + 1 - Q \sin^2 \theta_W) \sin^2 \theta_Q \\ z_{22} &= (m - Q \sin^2 \theta_W) \sin^2 \theta_Q + (m + 1 - Q \sin^2 \theta_W) \cos^2 \theta_Q \\ z_{12} &= \cos \theta_Q \sin \theta_Q \end{aligned} \quad (\text{A.7})$$

The matrix elements of potential matrix induced by the exchange of Z boson and photon are the following

$$\begin{aligned} V_{SS,SS} &= V_{AA,AA} = 0, \quad V_{SS,AA} = -\frac{\alpha}{4\cos^2\theta_W} \frac{e^{-m_Z r}}{r} \\ V_{\Delta^{(\frac{n+1}{2})}\Delta^{(-\frac{n+1}{2})}, \Delta^{(\frac{n+1}{2})}\Delta^{(-\frac{n+1}{2})}} &= -\frac{\alpha}{\cos^2\theta_W} \left( \frac{n}{2} - \frac{n+1}{2} \sin^2\theta_W \right)^2 \frac{e^{-m_Z r}}{r} - \frac{\alpha_{em} \left( \frac{n+1}{2} \right)^2}{r} \\ V_{\tilde{\Delta}_1^{(Q)}\tilde{\Delta}_1^{(-Q)}, \tilde{\Delta}_1^{(Q)}\tilde{\Delta}_1^{(-Q)}} &= -\frac{\alpha z_{11}^2}{\cos^2\theta_W} \frac{e^{-m_Z r}}{r} - \frac{\alpha_{em} Q^2}{r} \\ V_{\tilde{\Delta}_2^{(Q)}\tilde{\Delta}_2^{(-Q)}, \tilde{\Delta}_2^{(Q)}\tilde{\Delta}_2^{(-Q)}} &= -\frac{\alpha z_{22}^2}{\cos^2\theta_W} \frac{e^{-m_Z r}}{r} - \frac{\alpha_{em} Q^2}{r} \\ V_{\tilde{\Delta}_1^{(Q)}\tilde{\Delta}_1^{(-Q)}, \tilde{\Delta}_1^{(Q)}\tilde{\Delta}_2^{(-Q)}} &= -\frac{\alpha z_{11} z_{12}}{\cos^2\theta_W} \frac{e^{-m_Z r}}{r} = V_{\tilde{\Delta}_1^{(Q)}\tilde{\Delta}_1^{(-Q)}, \tilde{\Delta}_2^{(Q)}\tilde{\Delta}_1^{(-Q)}} \\ V_{\tilde{\Delta}_2^{(Q)}\tilde{\Delta}_2^{(-Q)}, \tilde{\Delta}_1^{(Q)}\tilde{\Delta}_2^{(-Q)}} &= -\frac{\alpha z_{22} z_{12}}{\cos^2\theta_W} \frac{e^{-m_Z r}}{r} = V_{\tilde{\Delta}_2^{(Q)}\tilde{\Delta}_2^{(-Q)}, \tilde{\Delta}_2^{(Q)}\tilde{\Delta}_1^{(-Q)}} \\ V_{\tilde{\Delta}_1^{(Q)}\tilde{\Delta}_2^{(-Q)}, \tilde{\Delta}_1^{(Q)}\tilde{\Delta}_2^{(-Q)}} &= -\frac{\alpha z_{11} z_{22}}{\cos^2\theta_W} \frac{e^{-m_Z r}}{r} - \frac{\alpha_{em} Q^2}{r} \\ V_{\tilde{\Delta}_1^{(Q)}\tilde{\Delta}_2^{(-Q)}, \tilde{\Delta}_2^{(Q)}\tilde{\Delta}_1^{(-Q)}} &= -\frac{\alpha z_{12}^2}{\cos^2\theta_W} \frac{e^{-m_Z r}}{r} \end{aligned}$$

These matrix elements are read off from Eq.(A.5) first by replacing the fields with their NR limits as given in Eq.(A.1) and then re-arranging them in the 2-particle fields  $\Phi_{ii'}^N$  and  $\Phi_{jj'}^C$ , so to match the  $V(\vec{r})$  term of the 2-particle effective action in Eq.(A.3).

**Matrix elements induced by  $W^\pm$  boson** Now the matrix elements induced by the exchange of W boson are the following. The charged current involving the charged components of the multiplet is

$$J_\mu^+ \supset ig \left( \sum_i a_{ii} \tilde{\Delta}_i^{(-Q)} \overleftrightarrow{\partial}_\mu \tilde{\Delta}_i^{(Q+1)} + \sum_{i \neq j} c_{ij} \tilde{\Delta}_i^{(-Q)} \overleftrightarrow{\partial}_\mu \tilde{\Delta}_j^{(Q+1)} \right)$$

Here,  $i, j = 1, 2$ .

We denote  $V_{j,m}^+ = \sqrt{(j-m)(j+m+1)}$  and  $V_{j,m}^- = \sqrt{(j+m)(j-m+1)}$ . Also  $V_{j,m}^+ = V_{j,m+1}^-$ . In the following we collect the the relevant matrix element of the potential matrix induced by the exchange of the  $W^\pm$  boson.

First let us consider the matrix elements induced by exchange of the W boson among the neutral pairs of charged components with the largest charge,  $Q = \frac{n+1}{2}$  ( $m = \frac{n}{2}$ ) and charge,  $Q-1 = \frac{n-1}{2}$  ( $m = \frac{n-2}{2}$ ) of the multiplet. They are

$$\begin{aligned} V_{\Delta^{(\frac{n+1}{2})} \Delta^{(-\frac{n+1}{2})}, \tilde{\Delta}_1^{(\frac{n-1}{2})} \tilde{\Delta}_1^{(-\frac{n-1}{2})}} &= -\frac{\alpha e^{-m_W r}}{r} (V_{\frac{n}{2}, \frac{n-2}{2}}^+)^2 \cos^2 \theta_{\frac{n-1}{2}} \\ V_{\Delta^{(\frac{n+1}{2})} \Delta^{(-\frac{n+1}{2})}, \tilde{\Delta}_2^{(\frac{n-1}{2})} \tilde{\Delta}_2^{(-\frac{n-1}{2})}} &= -\frac{\alpha e^{-m_W r}}{r} (V_{\frac{n}{2}, \frac{n-2}{2}}^+)^2 \sin^2 \theta_{\frac{n-1}{2}} \\ V_{\Delta^{(\frac{n+1}{2})} \Delta^{(-\frac{n+1}{2})}, \tilde{\Delta}_1^{(\frac{n-1}{2})} \tilde{\Delta}_2^{(-\frac{n-1}{2})}} &= -\frac{\alpha e^{-m_W r}}{r} (V_{\frac{n}{2}, \frac{n-2}{2}}^+)^2 \sin \theta_{\frac{n-1}{2}} \cos \theta_{\frac{n-1}{2}} \end{aligned}$$

Now we focus on the matrix elements induced by the exchange of W bosons among the neutral pairs of charged states with charge  $Q$  and  $Q+1$  of the multiplet.

$$\begin{aligned} V_{\tilde{\Delta}_1^{(Q)} \tilde{\Delta}_1^{(-Q)}, \tilde{\Delta}_1^{(Q+1)} \tilde{\Delta}_1^{(-Q-1)}} &= -\frac{\alpha e^{-m_W r}}{r} a_{11}^2, \quad V_{\tilde{\Delta}_1^{(Q)} \tilde{\Delta}_1^{(-Q)}, \tilde{\Delta}_2^{(Q+1)} \tilde{\Delta}_2^{(-Q-1)}} = -\frac{\alpha e^{-m_W r}}{r} c_{12}^2 \\ V_{\tilde{\Delta}_1^{(Q)} \tilde{\Delta}_1^{(-Q)}, \tilde{\Delta}_1^{(Q+1)} \tilde{\Delta}_2^{(-Q-1)}} &= V_{\tilde{\Delta}_1^{(Q)} \tilde{\Delta}_1^{(-Q)}, \tilde{\Delta}_2^{(Q+1)} \tilde{\Delta}_1^{(-Q-1)}} = -\frac{\alpha e^{-m_W r}}{r} a_{11} c_{12} \\ V_{\tilde{\Delta}_1^{(Q)} \tilde{\Delta}_2^{(-Q)}, \tilde{\Delta}_1^{(Q+1)} \tilde{\Delta}_1^{(-Q-1)}} &= V_{\tilde{\Delta}_2^{(Q)} \tilde{\Delta}_1^{(-Q)}, \tilde{\Delta}_1^{(Q+1)} \tilde{\Delta}_1^{(-Q-1)}} = -\frac{\alpha e^{-m_W r}}{r} a_{11} c_{21} \\ V_{\tilde{\Delta}_1^{(Q)} \tilde{\Delta}_2^{(-Q)}, \tilde{\Delta}_1^{(Q+1)} \tilde{\Delta}_2^{(-Q-1)}} &= V_{\tilde{\Delta}_2^{(Q)} \tilde{\Delta}_1^{(-Q)}, \tilde{\Delta}_1^{(Q+1)} \tilde{\Delta}_2^{(-Q-1)}} = -\frac{\alpha e^{-m_W r}}{r} a_{11} a_{22} \\ V_{\tilde{\Delta}_1^{(Q)} \tilde{\Delta}_2^{(-Q)}, \tilde{\Delta}_2^{(Q+1)} \tilde{\Delta}_1^{(-Q-1)}} &= V_{\tilde{\Delta}_2^{(Q)} \tilde{\Delta}_1^{(-Q)}, \tilde{\Delta}_2^{(Q+1)} \tilde{\Delta}_1^{(-Q-1)}} = -\frac{\alpha e^{-m_W r}}{r} c_{12} c_{21} \\ V_{\tilde{\Delta}_1^{(Q)} \tilde{\Delta}_2^{(-Q)}, \tilde{\Delta}_2^{(Q+1)} \tilde{\Delta}_2^{(-Q-1)}} &= V_{\tilde{\Delta}_2^{(Q)} \tilde{\Delta}_1^{(-Q)}, \tilde{\Delta}_2^{(Q+1)} \tilde{\Delta}_2^{(-Q-1)}} = -\frac{\alpha e^{-m_W r}}{r} c_{12} a_{22} \\ V_{\tilde{\Delta}_2^{(Q)} \tilde{\Delta}_2^{(-Q)}, \tilde{\Delta}_1^{(Q+1)} \tilde{\Delta}_2^{(-Q-1)}} &= V_{\tilde{\Delta}_2^{(Q)} \tilde{\Delta}_2^{(-Q)}, \tilde{\Delta}_2^{(Q+1)} \tilde{\Delta}_1^{(-Q-1)}} = -\frac{\alpha e^{-m_W r}}{r} c_{21} a_{22} \\ V_{\tilde{\Delta}_2^{(Q)} \tilde{\Delta}_2^{(-Q)}, \tilde{\Delta}_1^{(Q+1)} \tilde{\Delta}_1^{(-Q-1)}} &= -\frac{\alpha e^{-m_W r}}{r} c_{21}^2, \quad V_{\tilde{\Delta}_2^{(Q)} \tilde{\Delta}_2^{(-Q)}, \tilde{\Delta}_2^{(Q+1)} \tilde{\Delta}_2^{(-Q-1)}} = -\frac{\alpha e^{-m_W r}}{r} a_{22}^2 \end{aligned}$$

Here the factors  $a_{11}$ ,  $a_{22}$ ,  $c_{12}$  and  $c_{21}$  are

$$\begin{aligned} a_{11} &= V_{\frac{n}{2},m}^+ \cos \theta_Q \cos \theta_{Q+1} - V_{\frac{n}{2},-m-2}^+ \sin \theta_Q \sin \theta_{Q+1} \\ a_{22} &= V_{\frac{n}{2},m}^+ \sin \theta_Q \sin \theta_{Q+1} - V_{\frac{n}{2},-m-2}^+ \cos \theta_Q \cos \theta_{Q+1} \\ c_{12} &= V_{\frac{n}{2},m}^+ \cos \theta_Q \sin \theta_{Q+1} + V_{\frac{n}{2},-m-2}^+ \sin \theta_Q \cos \theta_{Q+1} \\ c_{21} &= V_{\frac{n}{2},m}^+ \sin \theta_Q \cos \theta_{Q+1} + V_{\frac{n}{2},-m-2}^+ \cos \theta_Q \sin \theta_{Q+1} \end{aligned}$$

The charged current involving  $S$  and  $A$  is

$$J_0^+ \supset \frac{ig}{2} (d_{S1} S \overleftrightarrow{\partial}_0 \tilde{\Delta}_1^+ - d_{S2} S \overleftrightarrow{\partial}_0 \tilde{\Delta}_2^+ - id_{A1} A \overleftrightarrow{\partial}_0 \tilde{\Delta}_1^+ + id_{A2} A \overleftrightarrow{\partial}_0 \tilde{\Delta}_2^+)$$

Here the factors are

$$\begin{aligned} d_{S1} &= V_{\frac{n}{2},-\frac{1}{2}}^+ \cos \theta_1 - V_{\frac{n}{2},-\frac{3}{2}}^+ \sin \theta_1 \\ d_{S2} &= V_{\frac{n}{2},-\frac{1}{2}}^+ \sin \theta_1 + V_{\frac{n}{2},-\frac{3}{2}}^+ \cos \theta_1 \\ d_{A1} &= V_{\frac{n}{2},-\frac{1}{2}}^+ \cos \theta_1 + V_{\frac{n}{2},-\frac{3}{2}}^+ \sin \theta_1 \\ d_{A2} &= V_{\frac{n}{2},-\frac{1}{2}}^+ \sin \theta_1 - V_{\frac{n}{2},-\frac{3}{2}}^+ \cos \theta_1 \end{aligned}$$

The matrix elements between the  $SS$ ,  $AA$  states and single charged states induced by the  $W$  boson are

$$\begin{aligned} V_{SS,\tilde{\Delta}_1^+\tilde{\Delta}_1^-} &= -\frac{\alpha e^{-m_W r}}{\sqrt{2}r} d_{S1}^2, \quad V_{SS,\tilde{\Delta}_2^+\tilde{\Delta}_2^-} = -\frac{\alpha e^{-m_W r}}{\sqrt{2}r} d_{S2}^2 \\ V_{SS,\tilde{\Delta}_1^+\tilde{\Delta}_2^-} &= V_{SS,\tilde{\Delta}_2^+\tilde{\Delta}_1^-} = -\frac{\alpha e^{-m_W r}}{\sqrt{2}r} d_{S1} d_{S2} \\ V_{AA,\tilde{\Delta}_1^+\tilde{\Delta}_1^-} &= -\frac{\alpha e^{-m_W r}}{\sqrt{2}r} d_{A1}^2, \quad V_{AA,\tilde{\Delta}_2^+\tilde{\Delta}_2^-} = -\frac{\alpha e^{-m_W r}}{\sqrt{2}r} d_{A2}^2 \\ V_{AA,\tilde{\Delta}_1^+\tilde{\Delta}_2^-} &= V_{AA,\tilde{\Delta}_2^+\tilde{\Delta}_1^-} = -\frac{\alpha e^{-m_W r}}{\sqrt{2}r} d_{A1} d_{A2} \end{aligned}$$

### A.3 The Annihilation Matrix Elements

In the non-relativistic limit, the  $2 \rightarrow 2$  S-wave annihilation channel is the most important channel. Therefore, we focus on the S-wave annihilation matrix elements. It can be derived from the gauge-scalar quartic couplings of the Lagrangian. The neutral sector and charged sector of quartic interactions are

$$\begin{aligned} \text{Neutral: } \mathcal{L} &\supset T_{W+W-} W_\mu^+ W^{-\mu} + T_{ZZ} Z_\mu Z^\mu + T_{AA} A_\mu A^\mu + T_{ZA} Z_\mu A^\mu \\ \text{Charged: } \mathcal{L} &\supset T_{W+W+} W_\mu^+ W^{+\mu} + T_{W+Z} W_\mu^+ Z^\mu + T_{W+A} W_\mu^+ A^\mu + \text{h.c.} \end{aligned} \quad (\text{A.8})$$

with

$$\begin{aligned} T_{W+W-} &= g^2 \Delta^\dagger (T^+ T^- + T^- T^+) \Delta, \quad T_{AA} = e^2 \Delta^\dagger \hat{Q}^2 \Delta \\ T_{ZZ} &= g^2 \cos^2 \theta_W \Delta^\dagger (T^3)^2 \Delta + gg' \cos \theta_W \sin \theta_W \Delta^\dagger T^3 Y \Delta + g'^2 \sin^2 \theta_W \Delta^\dagger Y^2 \Delta \\ T_{ZA} &= g^2 \sin 2\theta_W \Delta^\dagger (T^3)^2 \Delta + gg' \cos 2\theta_W \Delta^\dagger T^3 Y \Delta - g'^2 \sin 2\theta_W \Delta^\dagger Y^2 \Delta \\ T_{W+W+} &= g^2 \Delta^\dagger T^+ T^+ \Delta, \quad T_{W+Z} = g^2 \cos \theta_W \Delta^\dagger T^+ T^3 \Delta, \quad T^{W+A} = g^2 \sin \theta_W \Delta^\dagger T^+ T^3 \Delta \end{aligned} \quad (\text{A.9})$$



The S-wave annihilation matrix elements  $\Gamma^{VV}$  can be read from the terms in the effective action after integrating out the relativistic gauge bosons,

$$S_{\text{eff}} \supset \frac{i}{2\pi} \int d^4x d^3y \left( T_{VV}^\dagger(x) T_{VV}(x^0, \vec{y}) \right)_{ii',jj'} \delta^{(3)}(\vec{x}-\vec{y}) \equiv 2i \int d^4x d^3r \Gamma_{ii',jj'}^{(VV)} \delta^{(3)}(\vec{r}) \Phi_{ii'}^*(x, \vec{r}) \Phi_{jj'}(x, \vec{r})$$

after arranging mass eigenstates  $\tilde{\Delta}_i$ 's into 2-particle fields  $\Phi_{ii'}$  using their NR limits given in Eq.(A.1).

$\mathbf{\Gamma}_{ij,kl}^{(WW)}$  The matrix elements are,

$$\Gamma_{SS,SS}^{(WW)} = \frac{\pi\alpha^2}{2m_S^2} \left( j^2 + j - \frac{1}{4} \right)^2 = \Gamma_{SS,AA}^{(WW)} = \Gamma_{AA,AA}^{(WW)} \quad (\text{A.10})$$

Here,  $j = n/2$  is the isospin of the multiplet.

$$\begin{aligned} \Gamma_{\Delta^{(\frac{n+1}{2})}\Delta^{(-\frac{n+1}{2})},\Delta^{(\frac{n+1}{2})}\Delta^{(-\frac{n+1}{2})}}^{(WW)} &= \frac{\pi\alpha^2}{m_S^2} \frac{n^2}{4} \\ \Gamma_{\Delta^{(\frac{n+1}{2})}\Delta^{(-\frac{n+1}{2})},SS}^{(WW)} &= \frac{\pi\alpha^2}{\sqrt{2}m_S^2} j \left( j^2 + j - \frac{1}{4} \right) = \Gamma_{\Delta^{(\frac{n+1}{2})}\Delta^{(-\frac{n+1}{2})},AA}^{(WW)} \end{aligned} \quad (\text{A.11})$$

For convenience, let us define,  $R_{j,m} = (j^2 + j - m^2)$ .

$$\begin{aligned}
\Gamma_{\Delta^{(\frac{n+1}{2})}\Delta^{(-\frac{n+1}{2})},\tilde{\Delta}_1^{(Q)}\tilde{\Delta}_1^{(-Q)}}^{(WW)} &= \frac{\pi\alpha^2}{m_S^2} j(R_{j,m} \cos^2 \theta_Q + R_{j,-m-1} \sin^2 \theta_Q) \\
\Gamma_{\Delta^{(\frac{n+1}{2})}\Delta^{(-\frac{n+1}{2})},\tilde{\Delta}_2^{(Q)}\tilde{\Delta}_2^{(-Q)}}^{(WW)} &= \frac{\pi\alpha^2}{m_S^2} j(R_{j,m} \sin^2 \theta_Q + R_{j,-m-1} \cos^2 \theta_Q) \\
\Gamma_{\Delta^{(\frac{n+1}{2})}\Delta^{(-\frac{n+1}{2})},\tilde{\Delta}_1^{(Q)}\tilde{\Delta}_2^{(-Q)}}^{(WW)} &= \frac{\pi\alpha^2}{m_S^2} j(R_{j,m} - R_{j,-m-1}) \sin \theta_Q \cos \theta_Q \\
\Gamma_{SS,\tilde{\Delta}_1^{(Q)}\tilde{\Delta}_1^{(-Q)}}^{(WW)} &= \frac{\pi\alpha^2}{\sqrt{2}m_S^2} R_{j,-\frac{1}{2}} (R_{j,m} \cos^2 \theta_Q + R_{j,-m-1} \sin^2 \theta_Q) = \Gamma_{AA,\tilde{\Delta}_1^{(Q)}\tilde{\Delta}_1^{(-Q)}}^{(WW)} \\
\Gamma_{SS,\tilde{\Delta}_2^{(Q)}\tilde{\Delta}_2^{(-Q)}}^{(WW)} &= \frac{\pi\alpha^2}{\sqrt{2}m_S^2} R_{j,-\frac{1}{2}} (R_{j,m} \sin^2 \theta_Q + R_{j,-m-1} \cos^2 \theta_Q) = \Gamma_{AA,\tilde{\Delta}_2^{(Q)}\tilde{\Delta}_2^{(-Q)}}^{(WW)} \\
\Gamma_{SS,\tilde{\Delta}_1^{(Q)}\tilde{\Delta}_2^{(-Q)}}^{(WW)} &= \frac{\pi\alpha^2}{\sqrt{2}m_S^2} R_{j,-\frac{1}{2}} (R_{j,m} - R_{j,-m-1}) \sin \theta_Q \cos \theta_Q = \Gamma_{AA,\tilde{\Delta}_1^{(Q)}\tilde{\Delta}_2^{(-Q)}}^{(WW)} \\
\Gamma_{\tilde{\Delta}_1^{(Q)}\tilde{\Delta}_1^{(-Q)},\tilde{\Delta}_1^{(Q)}\tilde{\Delta}_1^{(-Q)}}^{(WW)} &= \frac{\pi\alpha^2}{m_S^2} (R_{j,m} \cos^2 \theta_Q + R_{j,-m-1} \sin^2 \theta_Q)^2 \\
\Gamma_{\tilde{\Delta}_2^{(Q)}\tilde{\Delta}_2^{(-Q)},\tilde{\Delta}_2^{(Q)}\tilde{\Delta}_2^{(-Q)}}^{(WW)} &= \frac{\pi\alpha^2}{m_S^2} (R_{j,m} \sin^2 \theta_Q + R_{j,-m-1} \cos^2 \theta_Q)^2 \\
\Gamma_{\tilde{\Delta}_1^{(Q)}\tilde{\Delta}_1^{(-Q)},\tilde{\Delta}_2^{(Q)}\tilde{\Delta}_2^{(-Q)}}^{(WW)} &= \frac{\pi\alpha^2}{m_S^2} (R_{j,m} \cos^2 \theta_Q + R_{j,-m-1} \sin^2 \theta_Q) \\
&\quad (R_{j,m} \sin^2 \theta_Q + R_{j,-m-1} \cos^2 \theta_Q) \\
\Gamma_{\tilde{\Delta}_1^{(Q)}\tilde{\Delta}_2^{(-Q)},\tilde{\Delta}_1^{(Q)}\tilde{\Delta}_2^{(-Q)}}^{(WW)} &= \frac{\pi\alpha^2}{m_S^2} (R_{j,m} - R_{j,-m-1})^2 \sin^2 \theta_Q \cos^2 \theta_Q \\
\Gamma_{\tilde{\Delta}_1^{(Q)}\tilde{\Delta}_1^{(-Q)},\tilde{\Delta}_1^{(Q)}\tilde{\Delta}_2^{(-Q)}}^{(WW)} &= \frac{\pi\alpha^2}{m_S^2} (R_{j,m} \cos^2 \theta_Q + R_{j,-m-1} \sin^2 \theta_Q) \\
&\quad (R_{j,m} - R_{j,-m-1}) \sin \theta_Q \cos \theta_Q \\
\Gamma_{\tilde{\Delta}_2^{(Q)}\tilde{\Delta}_2^{(-Q)},\tilde{\Delta}_1^{(Q)}\tilde{\Delta}_2^{(-Q)}}^{(WW)} &= \frac{\pi\alpha^2}{m_S^2} (R_{j,m} \sin^2 \theta_Q + R_{j,-m-1} \cos^2 \theta_Q) \\
&\quad (R_{j,m} - R_{j,-m-1}) \sin \theta_Q \cos \theta_Q
\end{aligned} \tag{A.12}$$

$\Gamma_{ij,kl}^{(ZZ)}$  First we define,  $V_m^{(z)} = m^2 \cos^2 \theta_W - m \sin^2 \theta_W + \frac{1}{4} \tan^2 \theta_W \sin^2 \theta_W$ .

$$\begin{aligned}
\Gamma_{\Delta^{(\frac{n+1}{2})}\Delta^{(-\frac{n+1}{2})},\Delta^{(\frac{n+1}{2})}\Delta^{(-\frac{n+1}{2})}}^{(ZZ)} &= \frac{2\pi\alpha^2}{m_S^2} (V_{\frac{n}{2}}^{(z)})^2 \\
\Gamma_{SS,SS}^{(ZZ)} &= \frac{\pi\alpha^2}{m_S^2} (V_{-\frac{1}{2}}^{(z)})^2 = \Gamma_{AA,AA}^{(ZZ)} = \Gamma_{SS,AA}^{(ZZ)}
\end{aligned} \tag{A.13}$$

$$\begin{aligned}
\Gamma_{\tilde{\Delta}_1^{(Q)} \tilde{\Delta}_1^{(-Q)}, \tilde{\Delta}_1^{(Q)} \tilde{\Delta}_1^{(-Q)}}^{(ZZ)} &= \frac{2\pi\alpha^2}{m_S^2} (V_m^{(z)} \cos^2 \theta_Q + V_{-m-1}^{(z)} \sin^2 \theta_Q)^2 \\
\Gamma_{\tilde{\Delta}_2^{(Q)} \tilde{\Delta}_2^{(-Q)}, \tilde{\Delta}_2^{(Q)} \tilde{\Delta}_2^{(-Q)}}^{(ZZ)} &= \frac{2\pi\alpha^2}{m_S^2} (V_m^{(z)} \sin^2 \theta_Q + V_{-m-1}^{(z)} \cos^2 \theta_Q)^2 \\
\Gamma_{\tilde{\Delta}_1^{(Q)} \tilde{\Delta}_1^{(-Q)}, \tilde{\Delta}_2^{(Q)} \tilde{\Delta}_2^{(-Q)}}^{(ZZ)} &= \frac{2\pi\alpha^2}{m_S^2} (V_m^{(z)} \cos^2 \theta_Q + V_{-m-1}^{(z)} \sin^2 \theta_Q) \\
&\quad (V_m^{(z)} \sin^2 \theta_Q + V_{-m-1}^{(z)} \cos^2 \theta_Q) \\
\Gamma_{\tilde{\Delta}_1^{(Q)} \tilde{\Delta}_2^{(-Q)}, \tilde{\Delta}_1^{(Q)} \tilde{\Delta}_2^{(-Q)}}^{(ZZ)} &= \frac{2\pi\alpha^2}{m_S^2} (V_m^{(z)} - V_{-m-1}^{(z)})^2 \sin^2 \theta_Q \cos^2 \theta_Q \\
\Gamma_{\tilde{\Delta}_1^{(Q)} \tilde{\Delta}_1^{(-Q)}, \tilde{\Delta}_1^{(Q)} \tilde{\Delta}_1^{(-Q)}}^{(ZZ)} &= \frac{2\pi\alpha^2}{m_S^2} (V_m^{(z)} \cos^2 \theta_Q + V_{-m-1}^{(z)} \sin^2 \theta_Q) \\
&\quad (V_m^{(z)} - V_{-m-1}^{(z)}) \sin \theta_Q \cos \theta_Q \\
\Gamma_{\tilde{\Delta}_1^{(Q)} \tilde{\Delta}_1^{(-Q)}, \tilde{\Delta}_1^{(Q)} \tilde{\Delta}_2^{(-Q)}}^{(ZZ)} &= \frac{2\pi\alpha^2}{m_S^2} (V_m^{(z)} \sin^2 \theta_Q + V_{-m-1}^{(z)} \cos^2 \theta_Q)^2 \\
&\quad (V_m^{(z)} - V_{-m-1}^{(z)}) \sin \theta_Q \cos \theta_Q \\
\Gamma_{\Delta^{(\frac{n+1}{2})} \Delta^{(-\frac{n+1}{2})}, \tilde{\Delta}_1^{(Q)} \tilde{\Delta}_1^{(-Q)}}^{(ZZ)} &= \frac{2\pi\alpha^2}{m_S^2} V_{\frac{n}{2}}^{(z)} (V_m^{(z)} \cos^2 \theta_Q + V_{-m-1}^{(z)} \sin^2 \theta_Q) \\
\Gamma_{\Delta^{(\frac{n+1}{2})} \Delta^{(-\frac{n+1}{2})}, \tilde{\Delta}_2^{(Q)} \tilde{\Delta}_2^{(-Q)}}^{(ZZ)} &= \frac{2\pi\alpha^2}{m_S^2} V_{\frac{n}{2}}^{(z)} (V_m^{(z)} \sin^2 \theta_Q + V_{-m-1}^{(z)} \cos^2 \theta_Q) \\
\Gamma_{\Delta^{(\frac{n+1}{2})} \Delta^{(-\frac{n+1}{2})}, \tilde{\Delta}_1^{(Q)} \tilde{\Delta}_1^{(-Q)}}^{(ZZ)} &= \frac{2\pi\alpha^2}{m_S^2} V_{\frac{n}{2}}^{(z)} (V_m^{(z)} - V_{-m-1}^{(z)}) \sin \theta_Q \cos \theta_Q \\
\Gamma_{SS, \tilde{\Delta}_1^{(Q)} \tilde{\Delta}_1^{(-Q)}}^{(ZZ)} &= \frac{\sqrt{2}\pi\alpha^2}{m_S^2} V_{-\frac{1}{2}}^{(z)} (V_m^{(z)} \cos^2 \theta_Q + V_{-m-1}^{(z)} \sin^2 \theta_Q) = \Gamma_{AA, \tilde{\Delta}_1^{(Q)} \tilde{\Delta}_1^{(-Q)}}^{(ZZ)} \\
\Gamma_{SS, \tilde{\Delta}_2^{(Q)} \tilde{\Delta}_2^{(-Q)}}^{(ZZ)} &= \frac{\sqrt{2}\pi\alpha^2}{m_S^2} V_{-\frac{1}{2}}^{(z)} (V_m^{(z)} \sin^2 \theta_Q + V_{-m-1}^{(z)} \cos^2 \theta_Q) = \Gamma_{AA, \tilde{\Delta}_2^{(Q)} \tilde{\Delta}_2^{(-Q)}}^{(ZZ)} \\
\Gamma_{SS, \tilde{\Delta}_1^{(Q)} \tilde{\Delta}_2^{(-Q)}}^{(ZZ)} &= \frac{\sqrt{2}\pi\alpha^2}{m_S^2} V_{-\frac{1}{2}}^{(z)} (V_m^{(z)} - V_{-m-1}^{(z)}) \sin \theta_Q \cos \theta_Q = \Gamma_{AA, \tilde{\Delta}_1^{(Q)} \tilde{\Delta}_2^{(-Q)}}^{(ZZ)}
\end{aligned}$$

$$\Gamma_{ij,kl}^{(\gamma\gamma)}$$

$$\begin{aligned}
\Gamma_{\Delta^{(\frac{n+1}{2})} \Delta^{(-\frac{n+1}{2})}, \Delta^{(\frac{n+1}{2})} \Delta^{(-\frac{n+1}{2})}}^{(\gamma\gamma)} &= \frac{2\pi\alpha_{em}^2}{m_S^2} \left(\frac{n+1}{2}\right)^2 \\
\Gamma_{\tilde{\Delta}_1^{(Q)} \tilde{\Delta}_1^{(-Q)}, \tilde{\Delta}_1^{(Q)} \tilde{\Delta}_1^{(-Q)}}^{(\gamma\gamma)} &= \frac{2\pi\alpha_{em}^2 Q^2}{m_S^2} = \Gamma_{\tilde{\Delta}_2^{(Q)} \tilde{\Delta}_2^{(-Q)}, \tilde{\Delta}_2^{(Q)} \tilde{\Delta}_2^{(-Q)}}^{(\gamma\gamma)} \\
\Gamma_{\Delta^{(\frac{n+1}{2})} \Delta^{(-\frac{n+1}{2})}, \tilde{\Delta}_1^{(Q)} \tilde{\Delta}_1^{(-Q)}}^{(\gamma\gamma)} &= \frac{2\pi\alpha_{em}^2}{m_S^2} \frac{(n+1)Q}{2} = \Gamma_{\Delta^{(\frac{n+1}{2})} \Delta^{(-\frac{n+1}{2})}, \tilde{\Delta}_2^{(Q)} \tilde{\Delta}_2^{(-Q)}}^{(\gamma\gamma)}
\end{aligned}$$

$\Gamma_{ij,kl}^{(\gamma Z)}$  Here we define,  $V_m^{(\gamma z)} = (m + \frac{1}{2}) (m \sin 2\theta_W - \sin^2 \theta_W \tan \theta_W)$ .

$$\begin{aligned}
\Gamma_{\Delta^{(\frac{n+1}{2})}\Delta^{(-\frac{n+1}{2})},\Delta^{(\frac{n+1}{2})}\Delta^{(-\frac{n+1}{2})}}^{(\gamma Z)} &= \frac{\pi\alpha^2}{m_S^2} (V_{\frac{n}{2}}^{(\gamma z)})^2 \\
\Gamma_{\tilde{\Delta}_1^{(Q)}\tilde{\Delta}_1^{(-Q)},\tilde{\Delta}_1^{(Q)}\tilde{\Delta}_1^{(-Q)}}^{(\gamma Z)} &= \frac{\pi\alpha^2}{m_S^2} (V_m^{(\gamma z)} \cos^2 \theta_Q + V_{-m-1}^{(\gamma z)} \sin^2 \theta_Q)^2 \\
\Gamma_{\tilde{\Delta}_2^{(Q)}\tilde{\Delta}_2^{(-Q)},\tilde{\Delta}_2^{(Q)}\tilde{\Delta}_2^{(-Q)}}^{(\gamma Z)} &= \frac{\pi\alpha^2}{m_S^2} (V_m^{(\gamma z)} \sin^2 \theta_Q + V_{-m-1}^{(\gamma z)} \cos^2 \theta_Q)^2 \\
\Gamma_{\tilde{\Delta}_1^{(Q)}\tilde{\Delta}_2^{(-Q)},\tilde{\Delta}_1^{(Q)}\tilde{\Delta}_2^{(-Q)}}^{(\gamma Z)} &= \frac{\pi\alpha^2}{m_S^2} (V_m^{(\gamma z)} - V_{-m-1}^{(\gamma z)})^2 \sin^2 \theta_Q \cos^2 \theta_Q \\
\Gamma_{\Delta^{(\frac{n+1}{2})}\Delta^{(-\frac{n+1}{2})},\tilde{\Delta}_1^{(Q)}\tilde{\Delta}_1^{(-Q)}}^{(\gamma Z)} &= \frac{\pi\alpha^2}{m_S^2} V_{\frac{n}{2}}^{(\gamma z)} (V_m^{(\gamma z)} \cos^2 \theta_Q + V_{-m-1}^{(\gamma z)} \sin^2 \theta_Q) \\
\Gamma_{\Delta^{(\frac{n+1}{2})}\Delta^{(-\frac{n+1}{2})},\tilde{\Delta}_2^{(Q)}\tilde{\Delta}_2^{(-Q)}}^{(\gamma Z)} &= \frac{\pi\alpha^2}{m_S^2} V_{\frac{n}{2}}^{(\gamma z)} (V_m^{(\gamma z)} \sin^2 \theta_Q + V_{-m-1}^{(\gamma z)} \cos^2 \theta_Q) \\
\Gamma_{\Delta^{(\frac{n+1}{2})}\Delta^{(-\frac{n+1}{2})},\tilde{\Delta}_1^{(Q)}\tilde{\Delta}_2^{(-Q)}}^{(\gamma Z)} &= \frac{\pi\alpha^2}{m_S^2} V_{\frac{n}{2}}^{(\gamma z)} (V_m^{(\gamma z)} - V_{-m-1}^{(\gamma z)}) \sin \theta_Q \cos \theta_Q \\
\Gamma_{\tilde{\Delta}_1^{(Q)}\tilde{\Delta}_1^{(-Q)},\tilde{\Delta}_1^{(Q)}\tilde{\Delta}_2^{(-Q)}}^{(\gamma Z)} &= \frac{\pi\alpha^2}{m_S^2} (V_m^{(\gamma z)} \cos^2 \theta_Q + V_{-m-1}^{(\gamma z)} \sin^2 \theta_Q) \\
&\quad (V_m^{(\gamma z)} - V_{-m-1}^{(\gamma z)}) \sin \theta_Q \cos \theta_Q \\
\Gamma_{\tilde{\Delta}_2^{(Q)}\tilde{\Delta}_2^{(-Q)},\tilde{\Delta}_1^{(Q)}\tilde{\Delta}_2^{(-Q)}}^{(\gamma Z)} &= \frac{\pi\alpha^2}{m_S^2} (V_m^{(\gamma z)} \sin^2 \theta_Q + V_{-m-1}^{(\gamma z)} \cos^2 \theta_Q) \\
&\quad (V_m^{(\gamma z)} - V_{-m-1}^{(\gamma z)}) \sin \theta_Q \cos \theta_Q
\end{aligned}$$

## References

- [1] T. Bringmann and C. Weniger, Phys. Dark Univ. **1**, 194 (2012) doi:10.1016/j.dark.2012.10.005 [arXiv:1208.5481 [hep-ph]].
- [2] M. Wood, J. Buckley, S. Digel, S. Funk, D. Nieto and M. A. Sanchez-Conde, arXiv:1305.0302 [astro-ph.HE].
- [3] J. Buckley *et al.*, arXiv:1310.7040 [astro-ph.HE].
- [4] M. Cirelli, arXiv:1511.02031 [astro-ph.HE].
- [5] S. Profumo, F. S. Queiroz and C. E. Yaguna, doi:10.1093/mnras/stw1600 arXiv:1602.08501 [astro-ph.HE].
- [6] K. Morà [H.E.S.S. Collaboration], arXiv:1512.00698 [astro-ph.HE].
- [7] H. Abdallah *et al.* [HESS Collaboration], Phys. Rev. Lett. **117**, no. 11, 111301 (2016) doi:10.1103/PhysRevLett.117.111301 [arXiv:1607.08142 [astro-ph.HE]].
- [8] H. Abdalla *et al.* [HESS Collaboration], Phys. Rev. Lett. **117**, no. 15, 151302 (2016) doi:10.1103/PhysRevLett.117.151302 [arXiv:1609.08091 [astro-ph.HE]].
- [9] M. Doro *et al.* [CTA Consortium Collaboration], Astropart. Phys. **43**, 189 (2013) doi:10.1016/j.astropartphys.2012.08.002 [arXiv:1208.5356 [astro-ph.IM]].
- [10] J. Carr *et al.* [CTA Collaboration], PoS ICRC **2015**, 1203 (2016) [arXiv:1508.06128 [astro-ph.HE]].

- [11] J. Conrad, arXiv:1610.03258 [astro-ph.HE].
- [12] V. Lefranc, G. A. Mamon and P. Panci, JCAP **1609**, no. 09, 021 (2016) doi:10.1088/1475-7516/2016/09/021 [arXiv:1605.02793 [astro-ph.HE]].
- [13] V. Lefranc, E. Moulin, P. Panci, F. Sala and J. Silk, JCAP **1609**, no. 09, 043 (2016) doi:10.1088/1475-7516/2016/09/043 [arXiv:1608.00786 [astro-ph.HE]].
- [14] A. Sommerfeld, Ann. Phys. **11**, 257 (1931)
- [15] J. Hisano, S. Matsumoto and M. M. Nojiri, Phys. Rev. D **67**, 075014 (2003) doi:10.1103/PhysRevD.67.075014 [hep-ph/0212022].
- [16] J. Hisano, S. Matsumoto and M. M. Nojiri, Phys. Rev. Lett. **92**, 031303 (2004) [hep-ph/0307216].
- [17] J. Hisano, S. Matsumoto, M. M. Nojiri and O. Saito, Phys. Rev. D **71**, 063528 (2005) [hep-ph/0412403].
- [18] J. Hisano, S. Matsumoto, O. Saito and M. Senami, Phys. Rev. D **73**, 055004 (2006) [hep-ph/0511118].
- [19] J. Hisano, S. Matsumoto, M. Nagai, O. Saito and M. Senami, Phys. Lett. B **646**, 34 (2007) doi:10.1016/j.physletb.2007.01.012 [hep-ph/0610249].
- [20] M. Cirelli, A. Strumia and M. Tamburini, Nucl. Phys. B **787**, 152 (2007) [arXiv:0706.4071 [hep-ph]].
- [21] M. Cirelli and A. Strumia, New J. Phys. **11**, 105005 (2009) [arXiv:0903.3381 [hep-ph]].
- [22] N. Arkani-Hamed, D. P. Finkbeiner, T. R. Slatyer and N. Weiner, Phys. Rev. D **79** (2009) 015014 [arXiv:0810.0713 [hep-ph]].
- [23] M. Lattanzi and J. I. Silk, Phys. Rev. D **79**, 083523 (2009) doi:10.1103/PhysRevD.79.083523 [arXiv:0812.0360 [astro-ph]].
- [24] L. Pieri, M. Lattanzi and J. Silk, Mon. Not. Roy. Astron. Soc. **399**, 2033 (2009) doi:10.1111/j.1365-2966.2009.15388.x [arXiv:0902.4330 [astro-ph.HE]].
- [25] R. Iengo, JHEP **0905**, 024 (2009) doi:10.1088/1126-6708/2009/05/024 [arXiv:0902.0688 [hep-ph]].
- [26] S. Cassel, J. Phys. G **37**, 105009 (2010) doi:10.1088/0954-3899/37/10/105009 [arXiv:0903.5307 [hep-ph]].
- [27] T. R. Slatyer, JCAP **1002** (2010) 028 [arXiv:0910.5713 [hep-ph]].
- [28] T. Hambye, F.-S. Ling, L. Lopez Honorez and J. Rocher, JHEP **0907** (2009) 090 [JHEP **1005** (2010) 066] [arXiv:0903.4010 [hep-ph]].
- [29] J. L. Feng, M. Kaplinghat and H. B. Yu, Phys. Rev. Lett. **104**, 151301 (2010) doi:10.1103/PhysRevLett.104.151301 [arXiv:0911.0422 [hep-ph]].
- [30] J. L. Feng, M. Kaplinghat and H. B. Yu, Phys. Rev. D **82**, 083525 (2010) doi:10.1103/PhysRevD.82.083525 [arXiv:1005.4678 [hep-ph]].
- [31] A. Hryczuk, R. Iengo and P. Ullio, JHEP **1103**, 069 (2011) doi:10.1007/JHEP03(2011)069 [arXiv:1010.2172 [hep-ph]].
- [32] A. Hryczuk and R. Iengo, JHEP **1201**, 163 (2012) Erratum: [JHEP **1206**, 137 (2012)] doi:10.1007/JHEP01(2012)163, 10.1007/JHEP06(2012)137 [arXiv:1111.2916 [hep-ph]].
- [33] M. Beneke, C. Hellmann and P. Ruiz-Femenia, JHEP **1303**, 148 (2013) Erratum: [JHEP **1310**, 224 (2013)] doi:10.1007/JHEP10(2013)224, 10.1007/JHEP03(2013)148 [arXiv:1210.7928 [hep-ph]].

- [34] S. Tulin, H. B. Yu and K. M. Zurek, *Phys. Rev. D* **87**, no. 11, 115007 (2013) doi:10.1103/PhysRevD.87.115007 [arXiv:1302.3898 [hep-ph]].
- [35] J. Fan and M. Reece, *JHEP* **1310**, 124 (2013) [arXiv:1307.4400 [hep-ph]].
- [36] T. Cohen, M. Lisanti, A. Pierce and T. R. Slatyer, *JCAP* **1310**, 061 (2013) [arXiv:1307.4082].
- [37] G. Ovanessian, T. R. Slatyer and I. W. Stewart, *Phys. Rev. Lett.* **114**, no. 21, 211302 (2015) doi:10.1103/PhysRevLett.114.211302 [arXiv:1409.8294 [hep-ph]].
- [38] M. Baumgart, I. Z. Rothstein and V. Vaidya, *Phys. Rev. Lett.* **114**, 211301 (2015) doi:10.1103/PhysRevLett.114.211301 [arXiv:1409.4415 [hep-ph]].
- [39] M. Beneke, C. Hellmann and P. Ruiz-Femenia, *JHEP* **1505**, 115 (2015) doi:10.1007/JHEP05(2015)115 [arXiv:1411.6924 [hep-ph]].
- [40] M. Cirelli, T. Hambye, P. Panci, F. Sala and M. Taoso, *JCAP* **1510**, no. 10, 026 (2015) [arXiv:1507.05519 [hep-ph]].
- [41] C. Garcia-Cely, A. Ibarra, A. S. Lamperstorfer and M. H. G. Tytgat, *JCAP* **1510**, no. 10, 058 (2015) [arXiv:1507.05536 [hep-ph]].
- [42] M. Aoki, T. Toma and A. Vicente, *JCAP* **1509**, 063 (2015) [arXiv:1507.01591 [hep-ph]].
- [43] E. Ma, *Phys. Rev. D* **73**, 077301 (2006) [hep-ph/0601225].
- [44] J. Kubo, E. Ma and D. Suematsu, *Phys. Lett. B* **642** (2006) 18 [hep-ph/0604114].
- [45] D. Aristizabal Sierra, J. Kubo, D. Restrepo, D. Suematsu and O. Zapata, *Phys. Rev. D* **79** (2009) 013011 [arXiv:0808.3340 [hep-ph]].
- [46] D. Suematsu, T. Toma and T. Yoshida, *Phys. Rev. D* **79** (2009) 093004 [arXiv:0903.0287 [hep-ph]].
- [47] A. Adulpravitchai, M. Lindner and A. Merle, *Phys. Rev. D* **80** (2009) 055031 [arXiv:0907.2147 [hep-ph]].
- [48] T. Toma and A. Vicente, *JHEP* **1401** (2014) 160 [arXiv:1312.2840, arXiv:1312.2840 [hep-ph]].
- [49] M. Klasen, C. E. Yaguna, J. D. Ruiz-Alvarez, D. Restrepo and O. Zapata, *JCAP* **1304**, 044 (2013) doi:10.1088/1475-7516/2013/04/044 [arXiv:1302.5298 [hep-ph]].
- [50] A. Vicente and C. E. Yaguna, *JHEP* **1502** (2015) 144 [arXiv:1412.2545 [hep-ph]].
- [51] E. Ma and D. Suematsu, *Mod. Phys. Lett. A* **24** (2009) 583 [arXiv:0809.0942 [hep-ph]].
- [52] S. S. C. Law and K. L. McDonald, *JHEP* **1309** (2013) 092 [arXiv:1305.6467 [hep-ph]].
- [53] B. Ren, K. Tsumura and X. G. He, *Phys. Rev. D* **84** (2011) 073004 [arXiv:1107.5879 [hep-ph]].
- [54] D. Restrepo, O. Zapata and C. E. Yaguna, *JHEP* **1311**, 011 (2013) doi:10.1007/JHEP11(2013)011 [arXiv:1308.3655 [hep-ph]].
- [55] T. A. Chowdhury and S. Nasri, *JHEP* **1512**, 040 (2015) doi:10.1007/JHEP12(2015)040 [arXiv:1506.00261 [hep-ph]].
- [56] A. Ahriche, K. L. McDonald and S. Nasri, *JHEP* **1606**, 182 (2016) doi:10.1007/JHEP06(2016)182 [arXiv:1604.05569 [hep-ph]].
- [57] A. Ahriche, A. Manning, K. L. McDonald and S. Nasri, *Phys. Rev. D* **94**, no. 5, 053005 (2016) doi:10.1103/PhysRevD.94.053005 [arXiv:1604.05995 [hep-ph]].
- [58] M. Cirelli, N. Fornengo and A. Strumia, *Nucl. Phys. B* **753** (2006) 178 [hep-ph/0512090].
- [59] F. S. Queiroz and C. E. Yaguna, *JCAP* **1602**, no. 02, 038 (2016) doi:10.1088/1475-7516/2016/02/038 [arXiv:1511.05967 [hep-ph]].
- [60] C. Garcia-Cely, M. Gustafsson and A. Ibarra, *JCAP* **1602**, no. 02, 043 (2016) doi:10.1088/1475-7516/2016/02/043 [arXiv:1512.02801 [hep-ph]].

- [61] S. S. AbdusSalam and T. A. Chowdhury, JCAP **1405**, 026 (2014) doi:10.1088/1475-7516/2014/05/026 [arXiv:1310.8152 [hep-ph]].
- [62] F. Nesti and G. Senjanović, Private communication, September, 2014
- [63] W. B. Lu and P. H. Gu, arXiv:1611.02106 [hep-ph].
- [64] M. Beneke and V. A. Smirnov, Nucl. Phys. B **522**, 321 (1998) doi:10.1016/S0550-3213(98)00138-2 [hep-ph/9711391].
- [65] Z. Zhang, Phys. Lett. B **734**, 188 (2014) doi:10.1016/j.physletb.2014.05.054 [arXiv:1307.2206 [hep-ph]].
- [66] R. Martinazzo, E. Bodo, F. A. Gianturco, Computer Physics Communications, **151**, 187 (2003). [http://dx.doi.org/10.1016/S0010-4655\(02\)00737-3](http://dx.doi.org/10.1016/S0010-4655(02)00737-3).
- [67] S. N. Ershov, J. S. Vaagen and M. V. Zhukov, Phys. Rev. C **84**, 064308 (2011). doi:10.1103/PhysRevC.84.064308
- [68] K. Blum, R. Sato and T. R. Slatyer, JCAP **1606**, no. 06, 021 (2016) doi:10.1088/1475-7516/2016/06/021 [arXiv:1603.01383 [hep-ph]].
- [69] P. A. R. Ade *et al.* [Planck Collaboration], Astron. Astrophys. **594**, A13 (2016) doi:10.1051/0004-6361/201525830 [arXiv:1502.01589 [astro-ph.CO]].
- [70] H. Baer, K. Y. Choi, J. E. Kim and L. Roszkowski, Phys. Rept. **555**, 1 (2015) doi:10.1016/j.physrep.2014.10.002 [arXiv:1407.0017 [hep-ph]].
- [71] J. Giedt, A. W. Thomas and R. D. Young, Phys. Rev. Lett. **103**, 201802 (2009) [arXiv:0907.4177 [hep-ph]].
- [72] D. S. Akerib *et al.*, arXiv:1608.07648 [astro-ph.CO].
- [73] E. Aprile *et al.* [XENON Collaboration], JCAP **1604**, no. 04, 027 (2016) doi:10.1088/1475-7516/2016/04/027 [arXiv:1512.07501 [physics.ins-det]].
- [74] M. Klasen, C. E. Yaguna and J. D. Ruiz-Alvarez, Phys. Rev. D **87**, 075025 (2013) doi:10.1103/PhysRevD.87.075025 [arXiv:1302.1657 [hep-ph]].
- [75] D. C. Kennedy and B. W. Lynn, Nucl. Phys. B **322**, 1 (1989). doi:10.1016/0550-3213(89)90483-5
- [76] M. E. Peskin and T. Takeuchi, Phys. Rev. D **46**, 381 (1992). doi:10.1103/PhysRevD.46.381
- [77] R. Barbieri, A. Pomarol, R. Rattazzi and A. Strumia, Nucl. Phys. B **703**, 127 (2004) doi:10.1016/j.nuclphysb.2004.10.014 [hep-ph/0405040].
- [78] C. Patrignani *et al.* [Particle Data Group Collaboration], Chin. Phys. C **40**, no. 10, 100001 (2016). doi:10.1088/1674-1137/40/10/100001
- [79] R. Barbieri, L. J. Hall and V. S. Rychkov, Phys. Rev. D **74**, 015007 (2006) doi:10.1103/PhysRevD.74.015007 [hep-ph/0603188].
- [80] H. Martinez, A. Melfo, F. Nesti, G. Senjanović, Phys. Rev. Lett. **106**, 191802 (2011). [arXiv:1101.3796 [hep-ph]].
- [81] A. Melfo, M. Nemevšek, F. Nesti, G. Senjanović, Y. Zhang, Phys. Rev. D **84** (2011) 034009. [arXiv:1105.4611 [hep-ph]].
- [82] T. A. Chowdhury, M. Nemevšek, G. Senjanović and Y. Zhang, JCAP **1202**, 029 (2012) [arXiv:1110.5334 [hep-ph]].
- [83] E. J. Chun, J. C. Park and S. Scopel, JCAP **1212**, 022 (2012) doi:10.1088/1475-7516/2012/12/022 [arXiv:1210.6104 [astro-ph.CO]].
- [84] C. A. Garcia-Cely, *Dark Matter Phenomenology in Scalar Extensions of the Standard Model* PhD thesis, Technische Universität München (TUM), (2014)

- [85] C. Garcia-Cely and A. Ibarra, JCAP **1309**, 025 (2013) doi:10.1088/1475-7516/2013/09/025 [arXiv:1306.4681 [hep-ph]].
- [86] A. Das and B. Dasgupta, arXiv:1611.04606 [hep-ph].
- [87] T. A. Chowdhury and S. Nasri, In preparation.
- [88] H. E. Logan and T. Pilkington, arXiv:1610.08835 [hep-ph].